X-RAY TELESCOPES
&
ASTROSAT SXT

K. P. Singh

IISER- Mohali

@COSPAR CBW 2019@IISER Mohali

PLAN

- X-ray Images using Focusing
- X-ray Optics – Basics
- Design of Telescopes
- Making of Telescopes
- Examples of X-ray Telescopes currently in use – **Chandra, XMM-Newton**
- Soft X-ray Telescope on AstroSat – its characteristics and performance

X-RAY IMAGES: ORION IN VISIBLE LIGHT AND X-RAYS

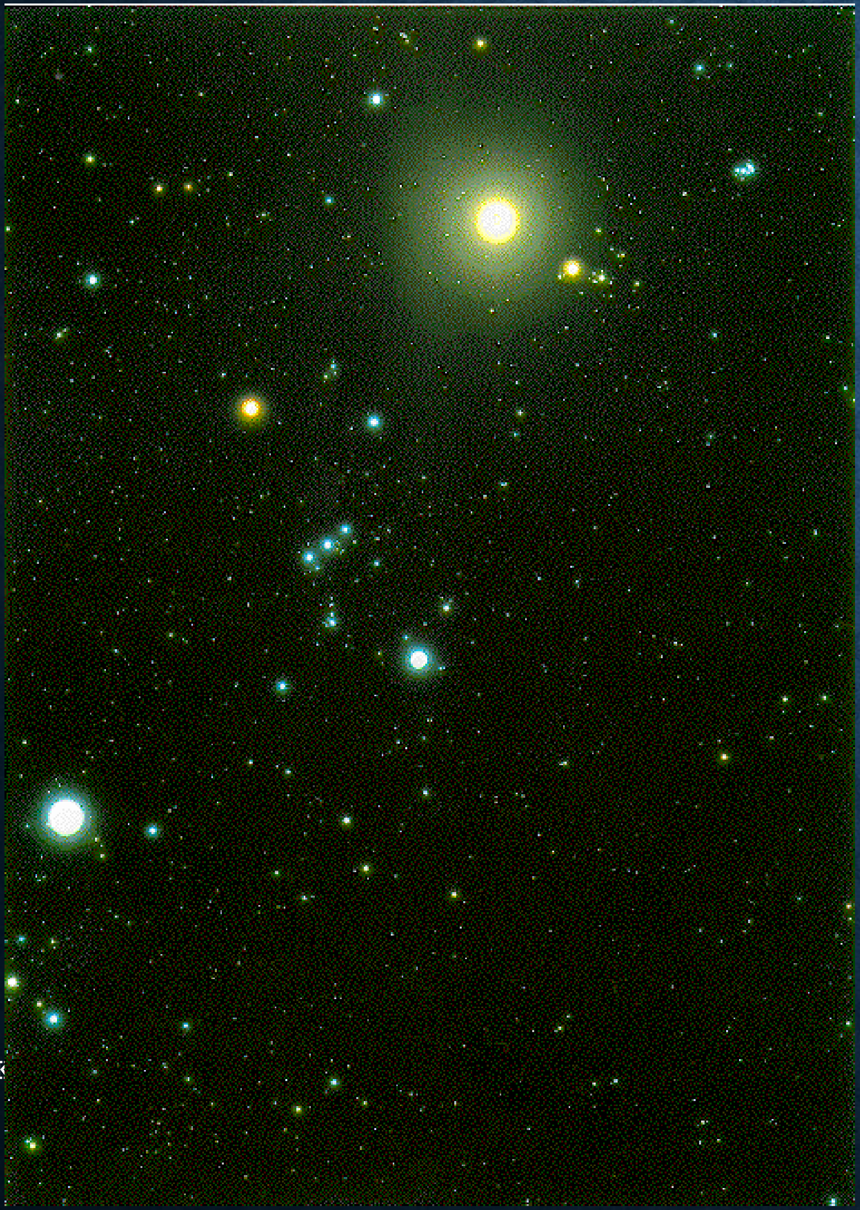

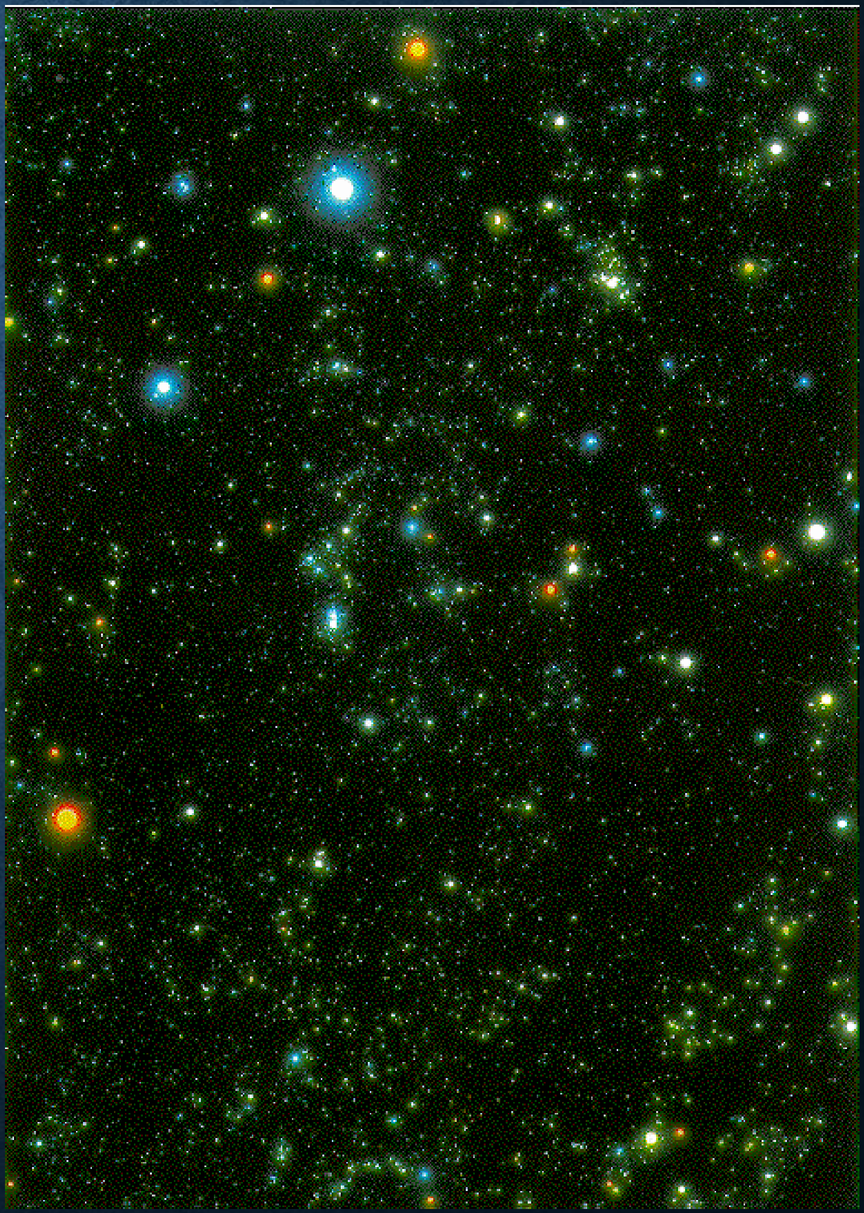

IMAGING THE HOT AND ENERGETIC UNIVERSE

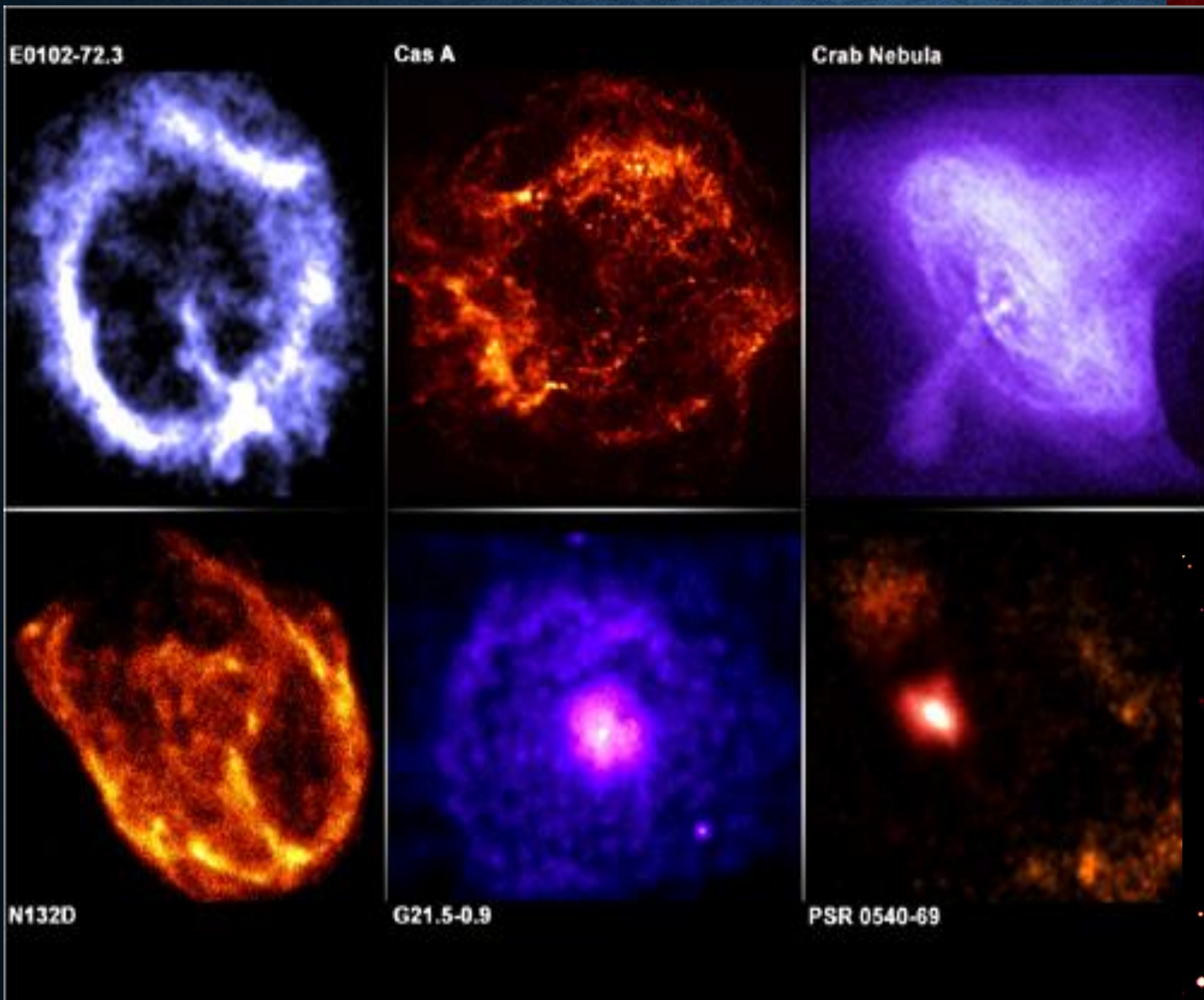

Sun, Stars, Supernova Remnants, the space between the Groups/ Clusters of Galaxies etc.

WHY DO WE USE X-RAY IMAGING?

- To achieve the best, 2-dimensional angular resolution to get *Accurate positions specially in crowded regions, image different parts of the same source for morphology*
- To collect or “gather” weak fluxes of photons – from faint and distant sources
- To concentrate/focus, so that the image photons interact in such a small region of the detector that non-X-ray background is negligible or small
- To serve with high spectral resolution dispersive spectrometers such as transmission or reflection gratings
- To simultaneously measure both the sources of interest, and the contaminating background using other regions of the detector.

X-RAY OPTICS: BASIC REQUIREMENT

We must make the X-rays Reflect

- Total External Reflection

Refractive Index for X-rays incident on a metal surface

- X-rays incident on a metal surface see most electrons as free

- Electron number density of plasma of electrons in a metal seen by the incident X-rays is

$$N_e = (Z-2)\rho/Am_p \text{ electrons/cm}^3$$

- Refractive Index of the plasma,

$$n = (1 - \omega_p^2/\omega^2)^{1/2} \text{, where}$$

$$\omega_p = 4\pi N_e e^2/m_e \text{ is the "plasma frequency"}$$

- $n < 1$ for X-rays ($\omega > \omega_p$) in a metal

SNELL'S LAW AND TOTAL EXTERNAL REFLECTION

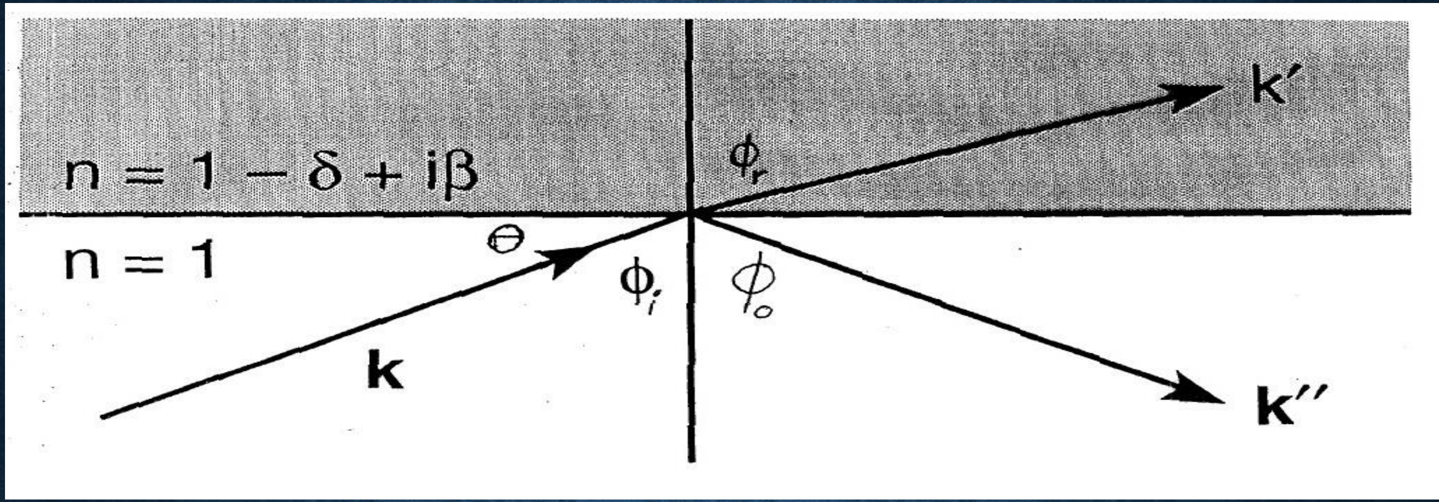

- Snell's law for refraction, $\sin\phi_i = n \sin \phi_r$

where ϕ is the standard angle of incidence from the surface normal, θ is the grazing angle from the surface.

- Since n < 1 for X-rays in a metal, X-rays bend away from the normal and most are absorbed
- When ϕ_i approaches 90°=X-rays undergo total internal ("external") reflection and we can write in terms of critical angle of reflection from the surface, $\cos\theta = (1 - \omega_p^2/\omega^2)^{1/2}$

CRITICAL GRAZING ANGLE

Using Taylor Series expansion on both sides

$1 - \theta^2/2 = 1 - 0.5\ \omega_p{}^2/\omega^2 \quad \rightarrow$

$\theta = \omega_p/\omega$ using $\omega = 2\pi c/\lambda$

$\theta = [(Z-2)\rho\ \lambda^2\ N\ e^2\ /\ (A\ m_e\ \pi\ c)]^{1/2}$

Therefore θ is proportional to $(Z)^{1/2}/E$

- The critical angle decreases inversely proportional to the energy.
- Higher Z materials reflect higher energies, for fixed grazing angles.
- Higher Z materials have a larger critical angle at any energy.

For heavy elements, Ni, Au, Pt, Ir, etc. Z / A = 0.5, and

$\theta = 5.6\ \lambda\ \rho^{1/2}$ arcmin

(λ is in Angstroms, and ρ is in gm/cm^3) < 1 deg.

CRITICAL GRAZING ANGLE

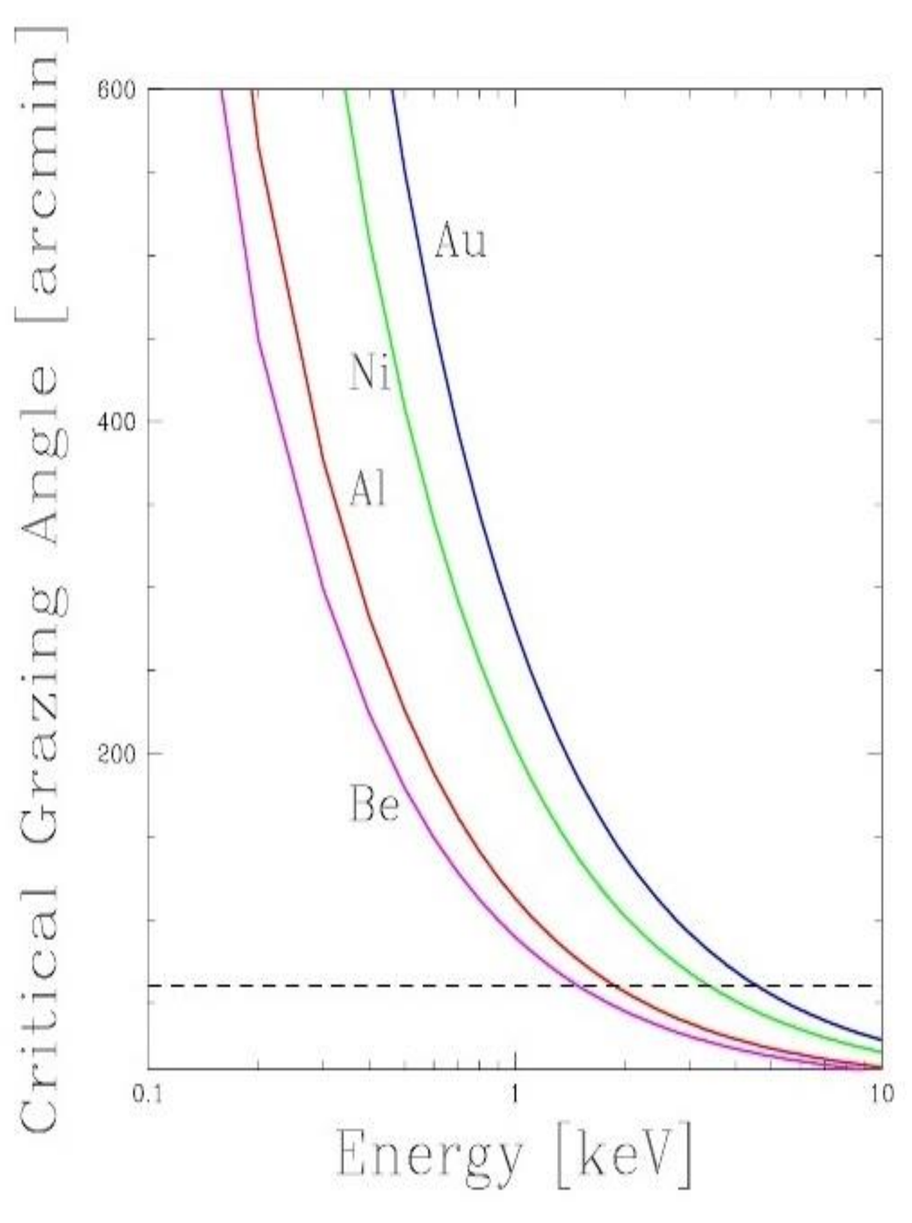

X-RAY REFLECTIVITIES OF METALS

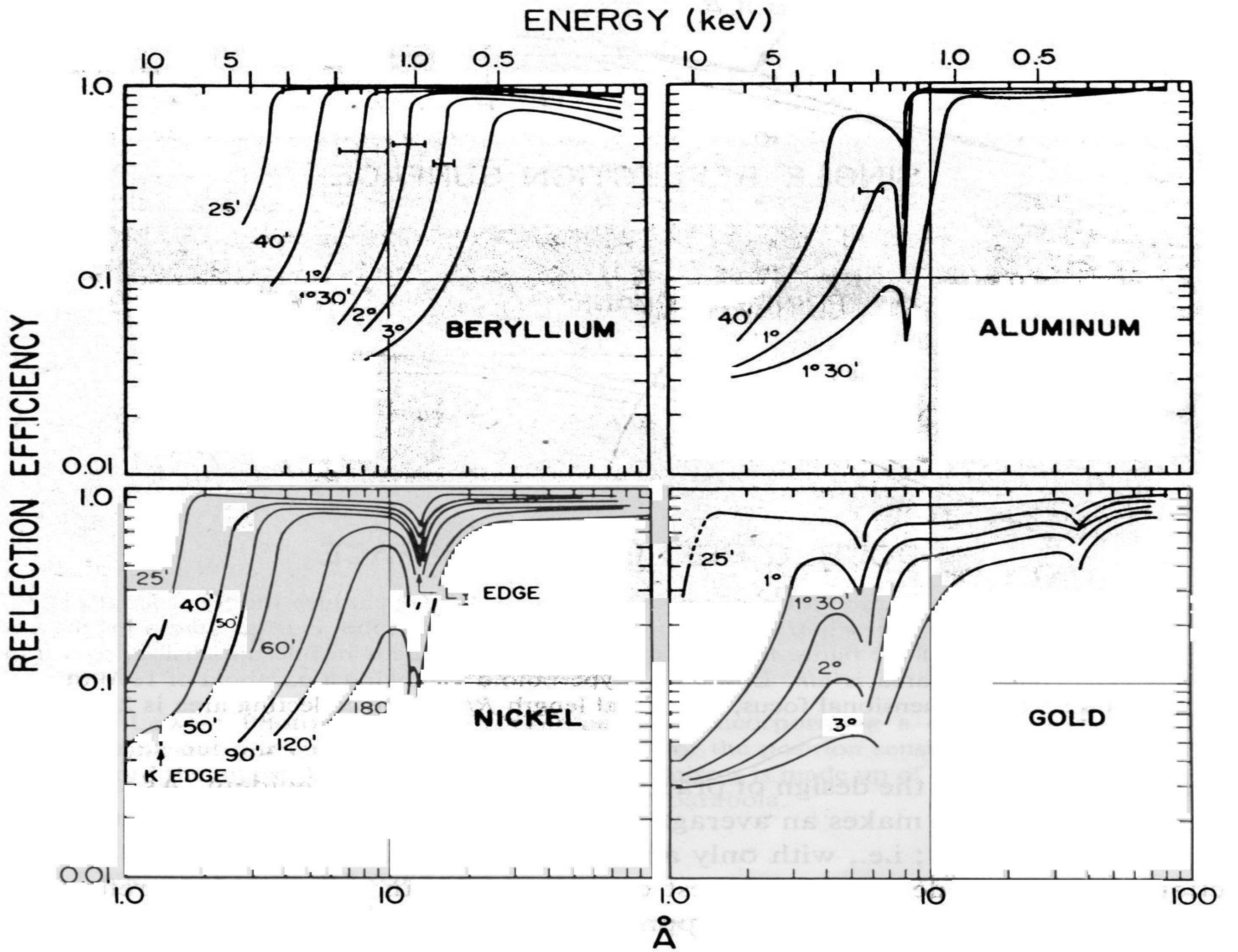

Fig. 2.20 Theoretical reflection efficiencies of Be($Z=4$), Al($Z=13$), Ni($Z=28$), and Au($Z=79$) surfaces as a function of energy or wavelength, for various grazing angles. Actual mirrors are less efficient, depending sensitively on the surface finish. The critical angle for a given energy may be defined as the angle at which the reflectivity drops below some arbitrary level, e.g. 10 %. The complexities of the curves are due to absorption edge effects.

KPSingh

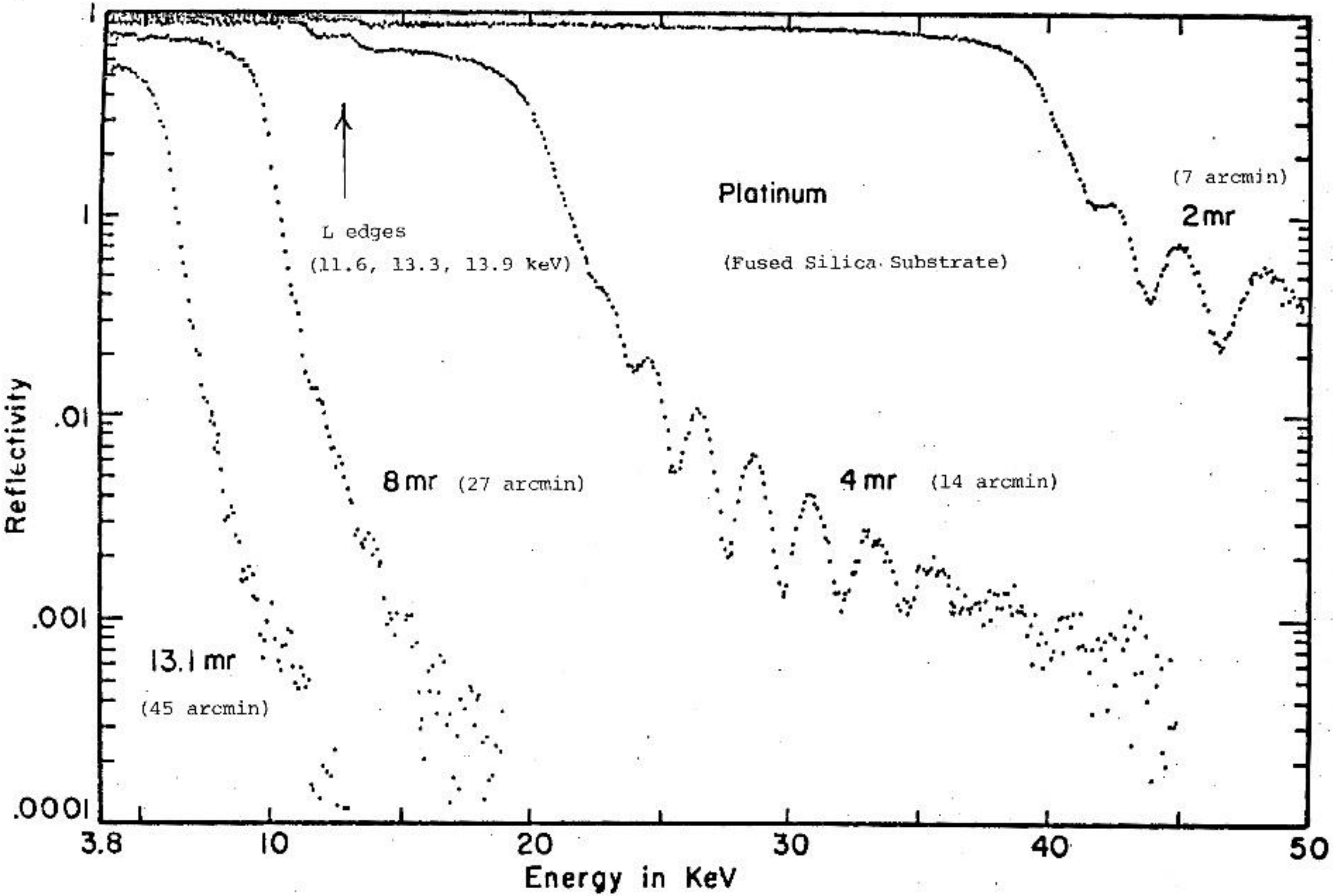

Figure 3.2 The reflectivity of a platinum coated mirror as a function of energy and grazing angle.

X-RAY REFLECTION: NOT THE END OF THE STORY

- Three Significant effects remain:

1. The surfaces are not infinitely smooth.

This gives rise to the complex subject of X-ray scattering. Scattering cannot be treated *exactly, one must consider a statistical description* of the surface roughness.

Key Features:

- Scattering increases as E^2
- In plane scattering dominates by factor **1/sinθ**

2. WE GENERALLY DO NOT HAVE A PERFECT INTERFACE FROM A VACUUM TO AN INFINITELY THICK REFLECTING LAYER.

We must consider:

- The mirror substrate material; e.g., Zerodur for Chandra
- A thin binding layer, e.g., Chromium, to hold the heavy metallic coating to the glass
- The high Z metal coating; e.g., Iridium for Chandra
- An unwanted but inadvertent overcoat of molecular contaminants

Feature: Interference can cause oscillations in reflectivity.

3. PREPARATION OF COATING AFFECTS REFLECTIVITY THROUGH THE DEPENDENCE ON DENSITY.

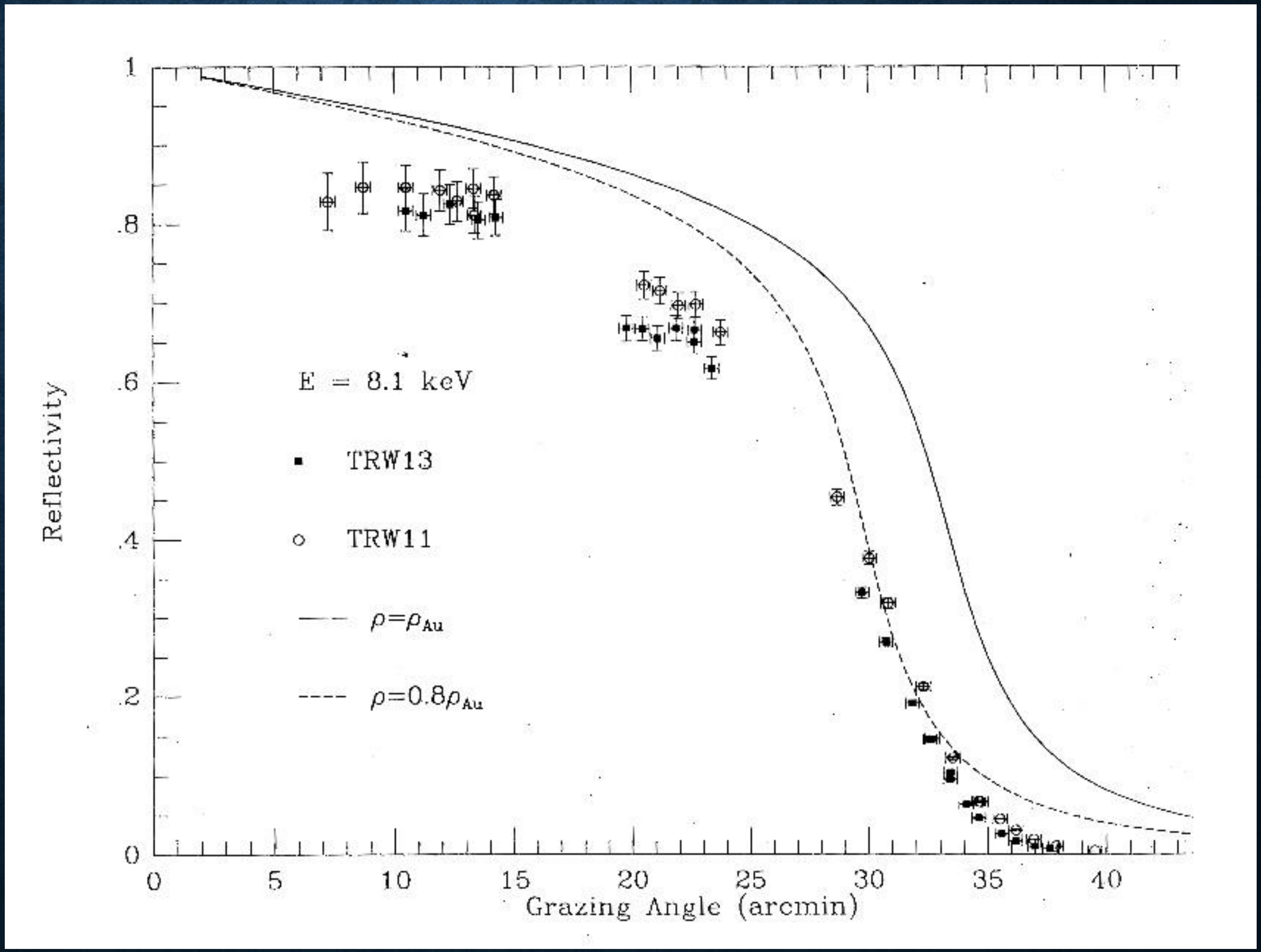

KPSingh

X-RAY OPTICS: BASIC REQUIREMENTS

1. We must make the X-rays Reflect
   - Total External Reflection

2. We must make the X-rays form an Image
   - Control Mirror Figure
   - Control Scattering

FOCUSING BY CURVED PARABOLA PLATES

1-D focusing

- Rays parallel to the parabola axis are focused to a point.
- Off-axis, the blur circle increases linearly with the angle.

PARABOLIC OPTICS

Horizontal and vertical focusing are separated at grazing incidence. **$f_m = (R \sin\theta)/2$; $f_s = R/(2\sin\theta)$**

Decoupling the meridional and sagittal focusing elements

Using parabolic sheet mirrors (Parabolas of translation) with axes of revolution perpendicular to each other and using a stack of mirrors.

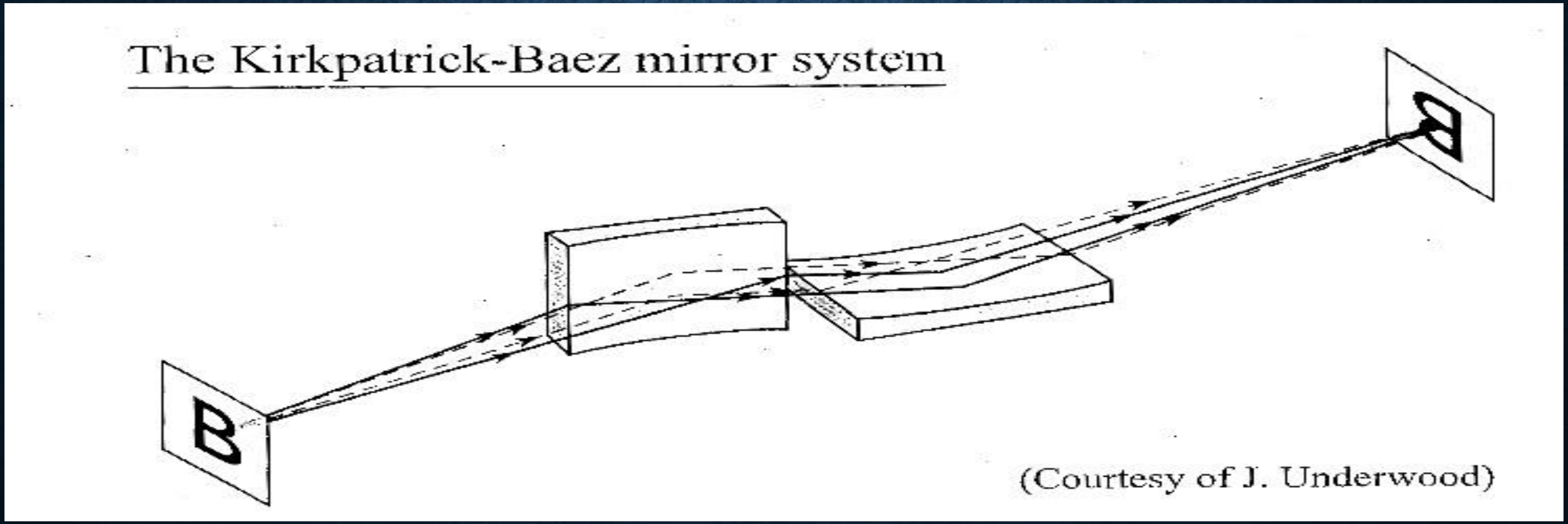

KIRKPATRICK-BAEZ (1948) OPTICS FOR X-RAYS

The first ever 2-D X-ray image in the Lab.

Effective area=$r^2 fm(\alpha lh)$, r=reflectivity,f=fraction of light emerging from the front mirror and intercepted by the rear mirror, m=no. of plates in the front mirror.

Ray tracing → spatial resolution is 5-10 arcsecs on axis and 1 arcmin for rays 1 deg off axis.

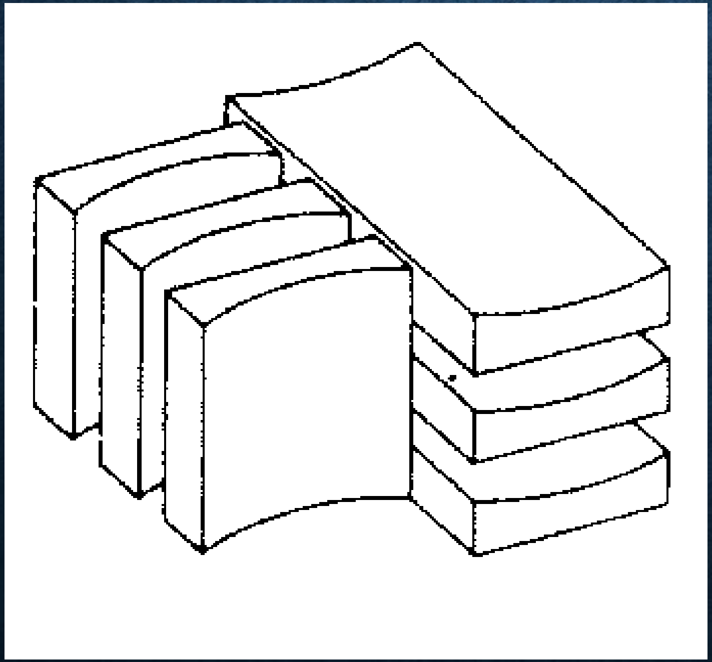

Stacking to increase area

WOLTER'S CONFIGURATIONS

Wolter, H. 1952, *Ann. Physik 10, 94;ibid. 286;*

Giacconi, R. & Rossi, B. 1960, *J. Geophys. Res. 65, 773*

- A parabola of revolution (rotating the parabola around its central axis) will focus only the on-axis rays. Off-axis rays (off-axis by angle d will focus on a ring of radius Fd.
- A Paraboloid produces a perfect focus for on-axis rays.
- Off-axis it gives a coma blur size proportional to the distance off-axis.
- Wolter's classic paper proved two reflections were needed, and considered configurations of conics to eliminate coma.
- Basic Principle: The optical path to the image must be identical for all rays incident on the telescope, in order to achieve perfect imaging.
- Wolter derived three possible Geometries.

WOLTER'S CONFIGURATIONS

Wolter (1952) Ann. Phys., NY, 10, 94 & 286

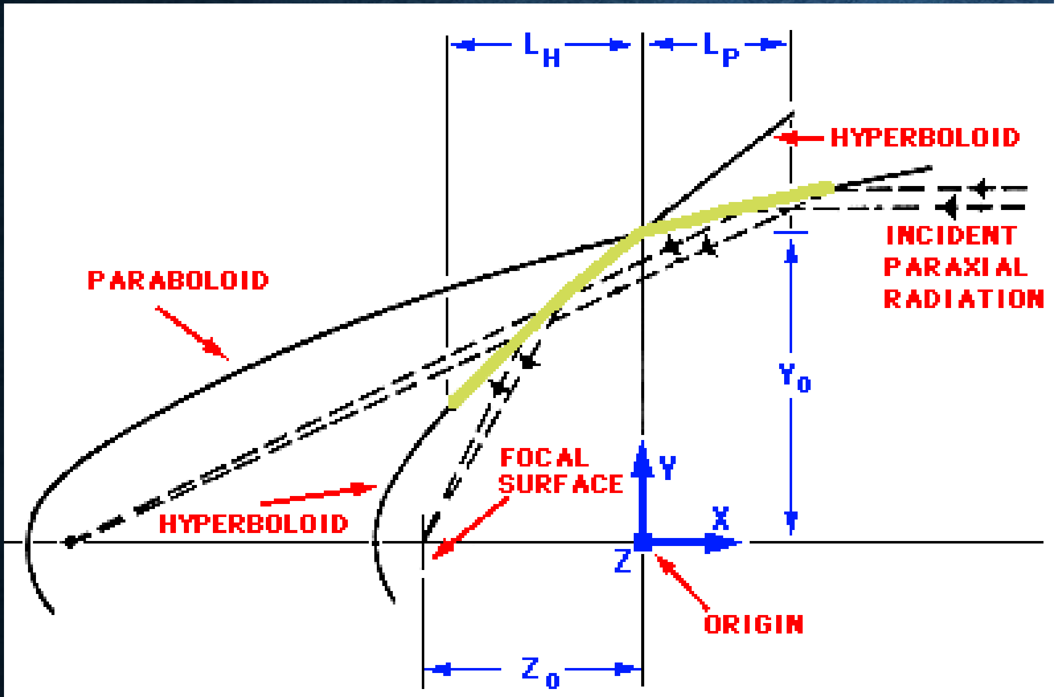

Type I

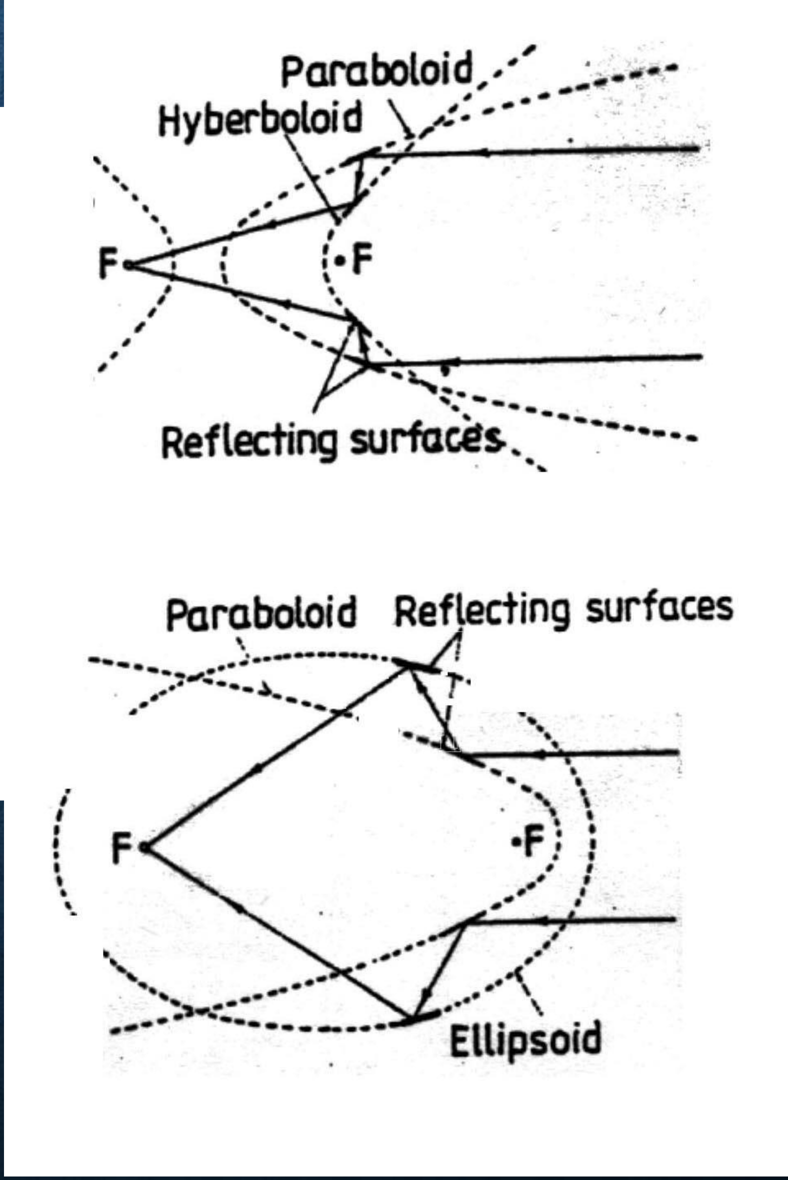

KPSingh

Types II, III

WOLTER-I CONFIGURATION

The Type I or the Paraboloid-Hyperboloid is overwhelmingly most useful in cosmic X-ray astronomy:

- Shortest Focal length to aperture ratio. This has been a key discriminator as we are always trying to maximize the collecting area to detect weak fluxes, but with relatively severe restrictions on length (and diameter) imposed by available space vehicles.
- For resolved sources, the shorter focal length concentrates a given spatial element of surface brightness onto a smaller detector area, hence gives a better signal to noise ratio against the non-X-ray detector background.

X-Ray Mirrors: Paraboloid-Hyperboloid

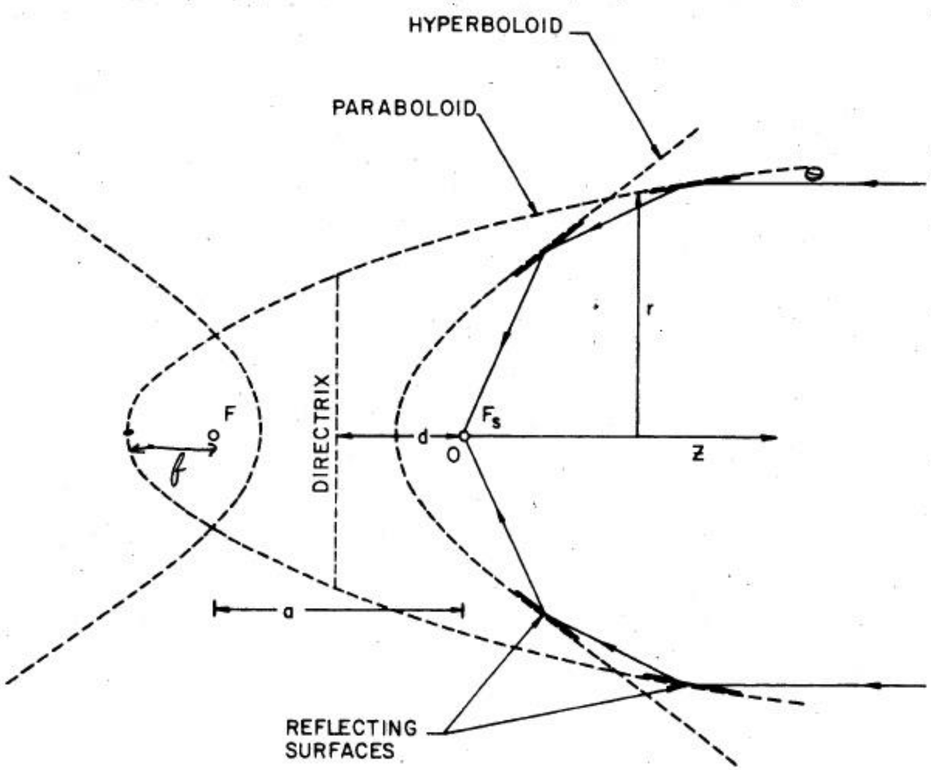

FIGURE 3 THE PRINCIPLE OF THE WOLTER TYPE I TELESCOPE. THE TELESCOPE FOCUS IS AT F_S. THE FOCUS OF THE PARABOLOID IS AT THE SECOND FOCUS OF THE HYPERBOLOID.

Advantages of intersecting P and H surfaces: mounting, nesting, and vignetting considerations. For replicated mirrors, the P and H figures are typically polished on a single mandrel and the pair formed as a single piece.

One requirement of the shorter focal length is that it puts more demand on having a detector with smaller spatial resolution in order to sample the image.

CHANDRA'S 4 NESTED X-RAY TELESCOPES

Increasing the Collecting area

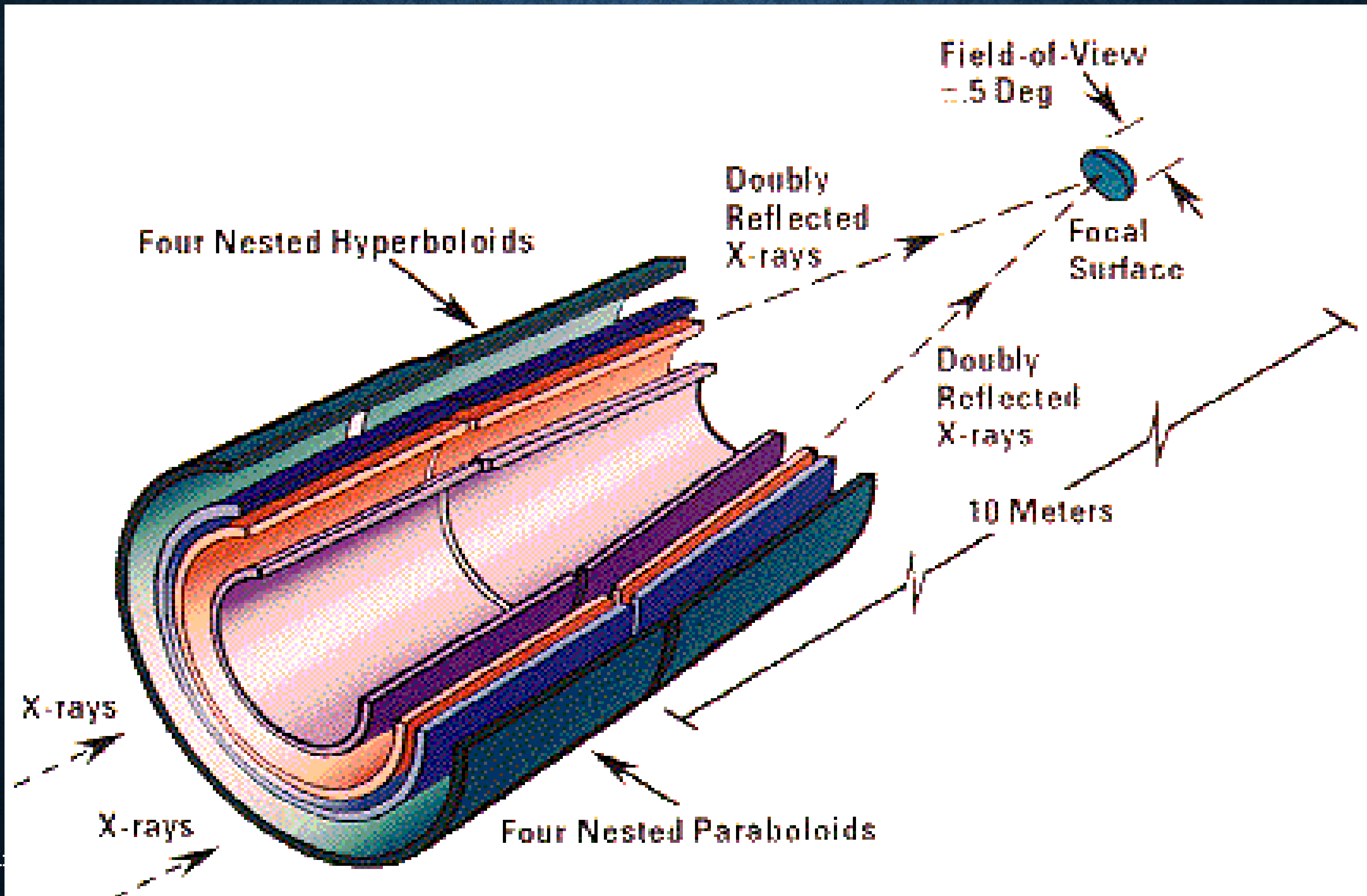

Mirror elements are 0.8 m long and from 0.6 m to 1.2 m diameter

GRINDING AND POLISHING (CHANDRA)

Wolter Type 1

KPSingh

MIRRORS FOR CXO

CHANDRA X-RAY OBSERVATORY

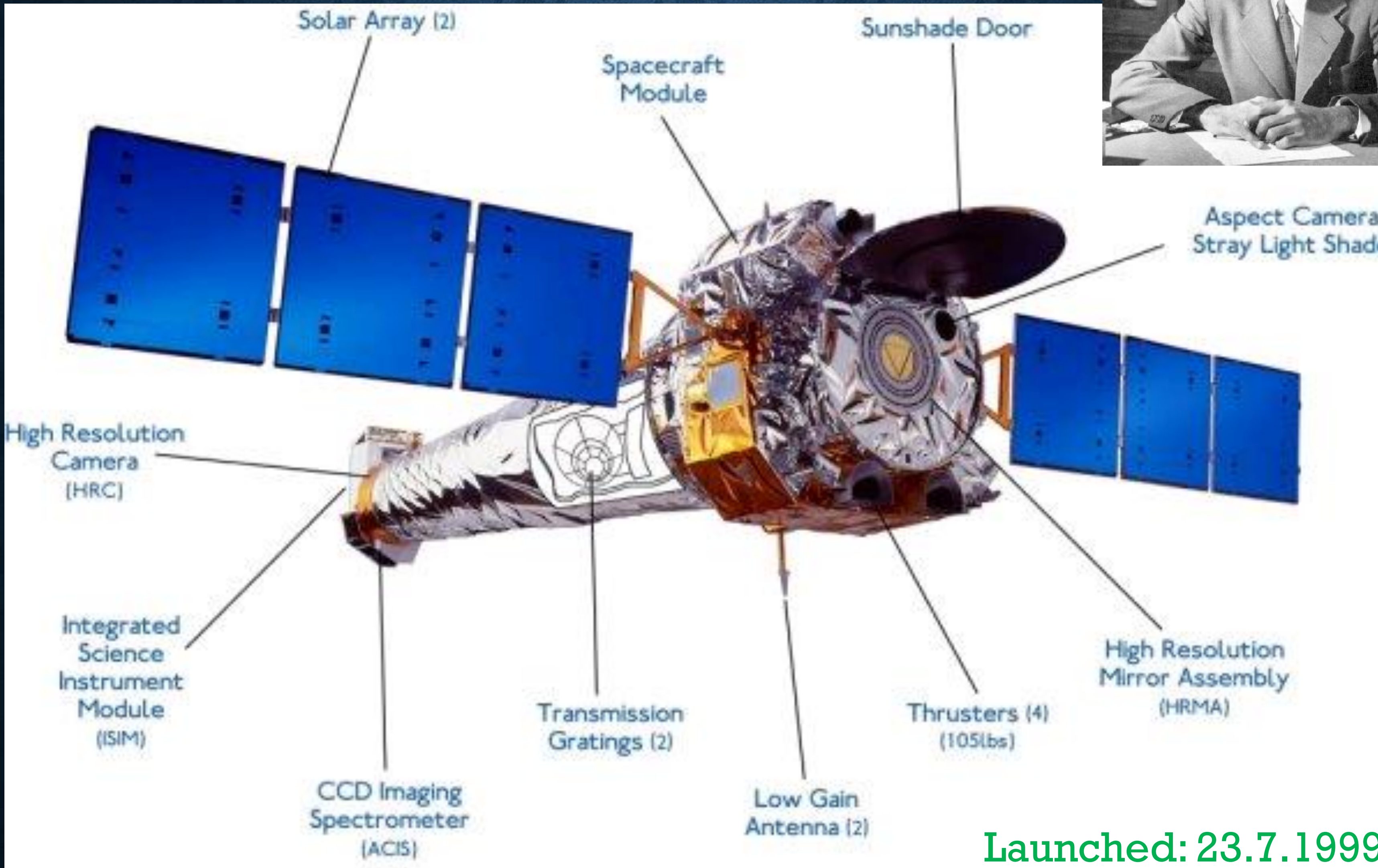

Launched: 23.7.1999

84 cm long mirrors; 10 m focal length; 1484 Kgs (mirrors only);

Area =1145 cm^2 (Geom.) and 0.5 arcsec resolution (FWHM)

REPLICATION TECHNOLOGIES

XMM – Newton: Electroforming Technique

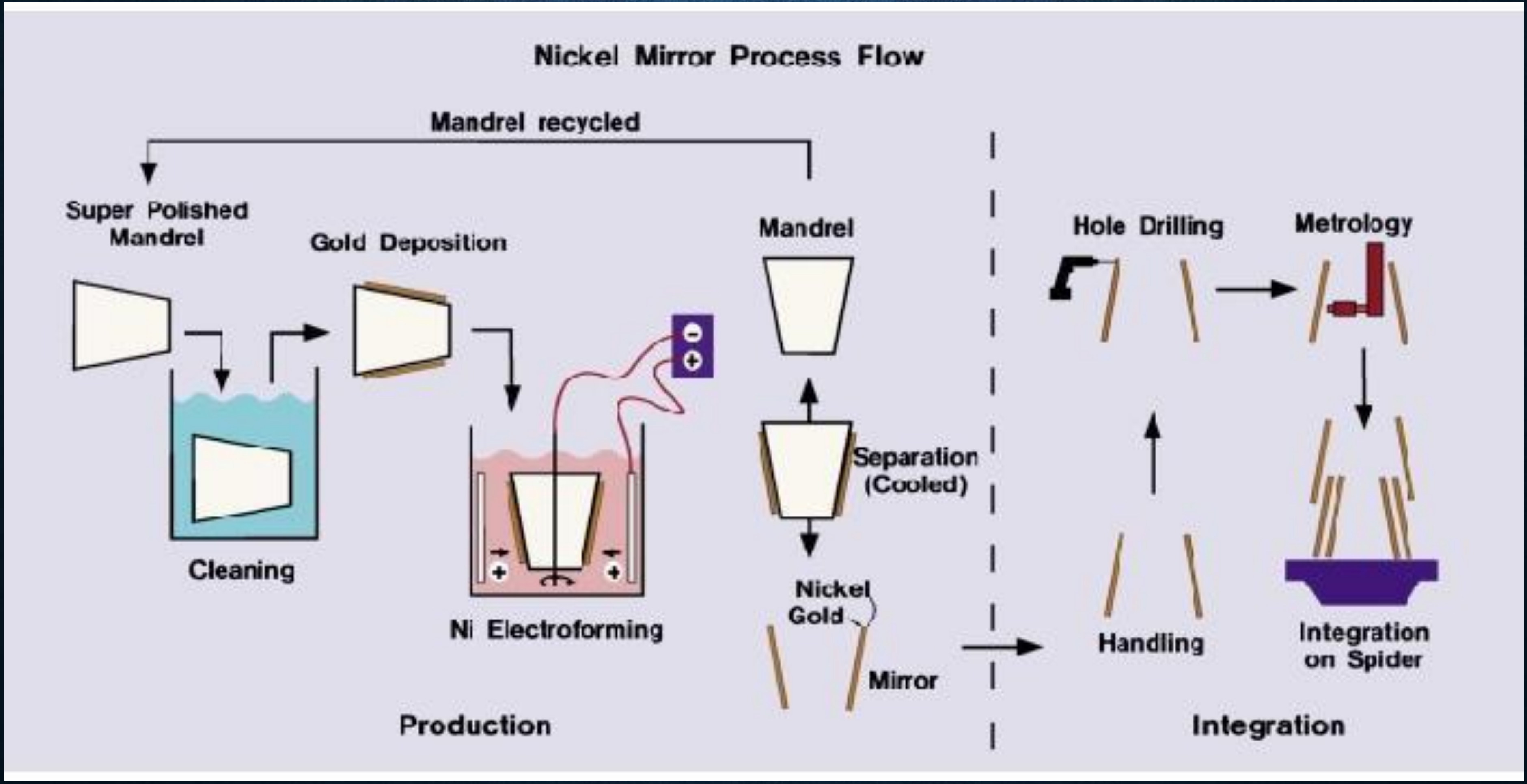

X-RAY MULTI MIRROR (XMM)-NEWTON

Wolter Type 1 with 58 mirror shells of Nickel coated with Gold.

Focal Length: 750 cm

Outermost Mirror Dia:70cm

Innermost Mirror Dia:31.8cm

Axial Mirror Length paraboloid + hyperboloid:

60 cm

Wall Thickness:

1.07-0.47 mm

Min. Packing Distance: 3 mm

Mirror Module Mass: 437 kg

Angular Resolution, Half Energy Width

15 arc seconds, 0.1-10 keV

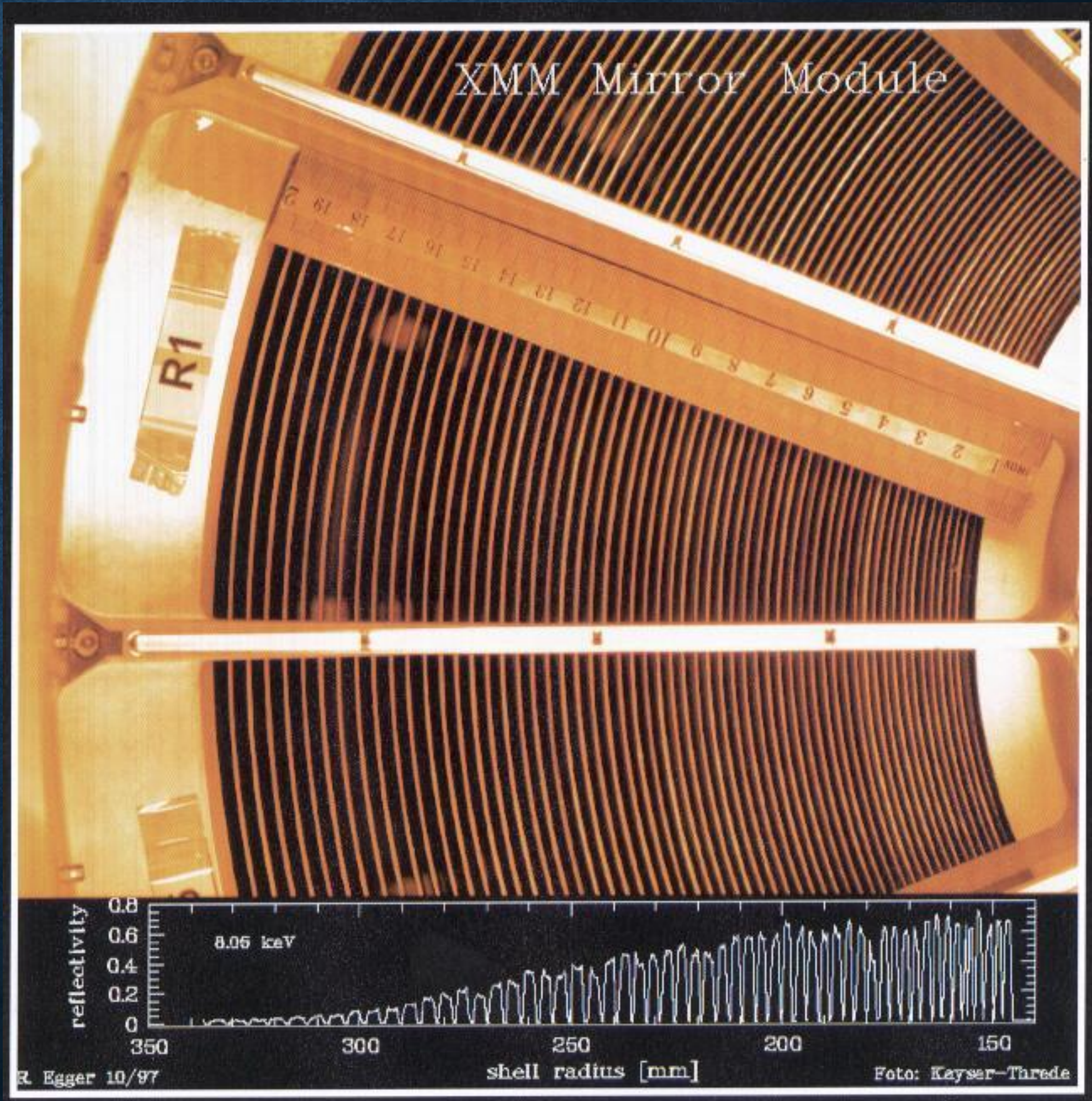

XMM-NEWTON X-RAY TELESCOPE

Launched on 10th Dec. 1999 by ESA -- the largest X-ray observatory : 3 X-ray Telescopes (1 is shown below)

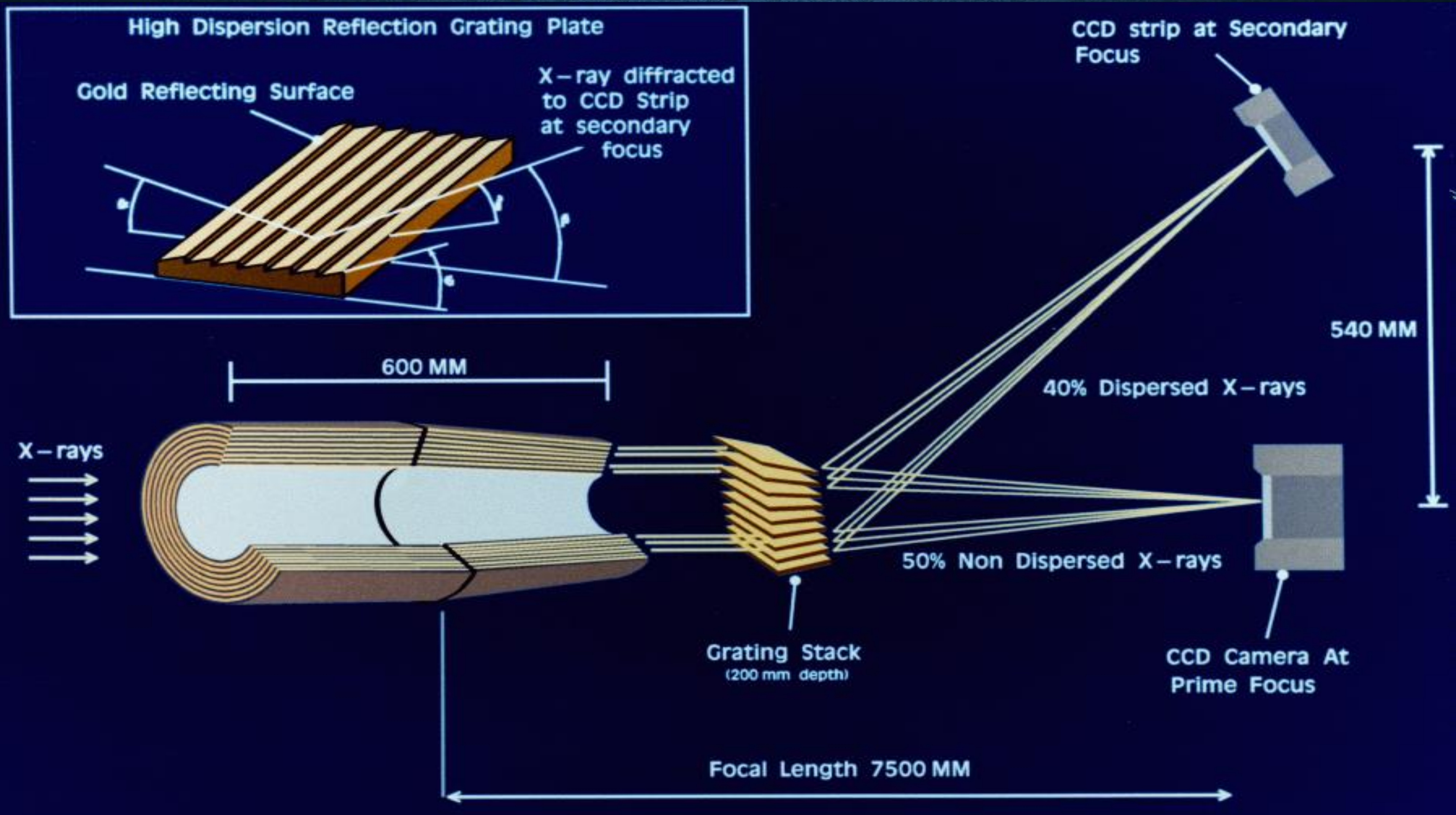

EPOXY REPLICATION PROCESS FOR FLAT FOILS

Conical Approximation to Wolter I:
Used for making Suzaku mirrors and adopted for a soft X-ray telescope for AstroSat

KPSingh

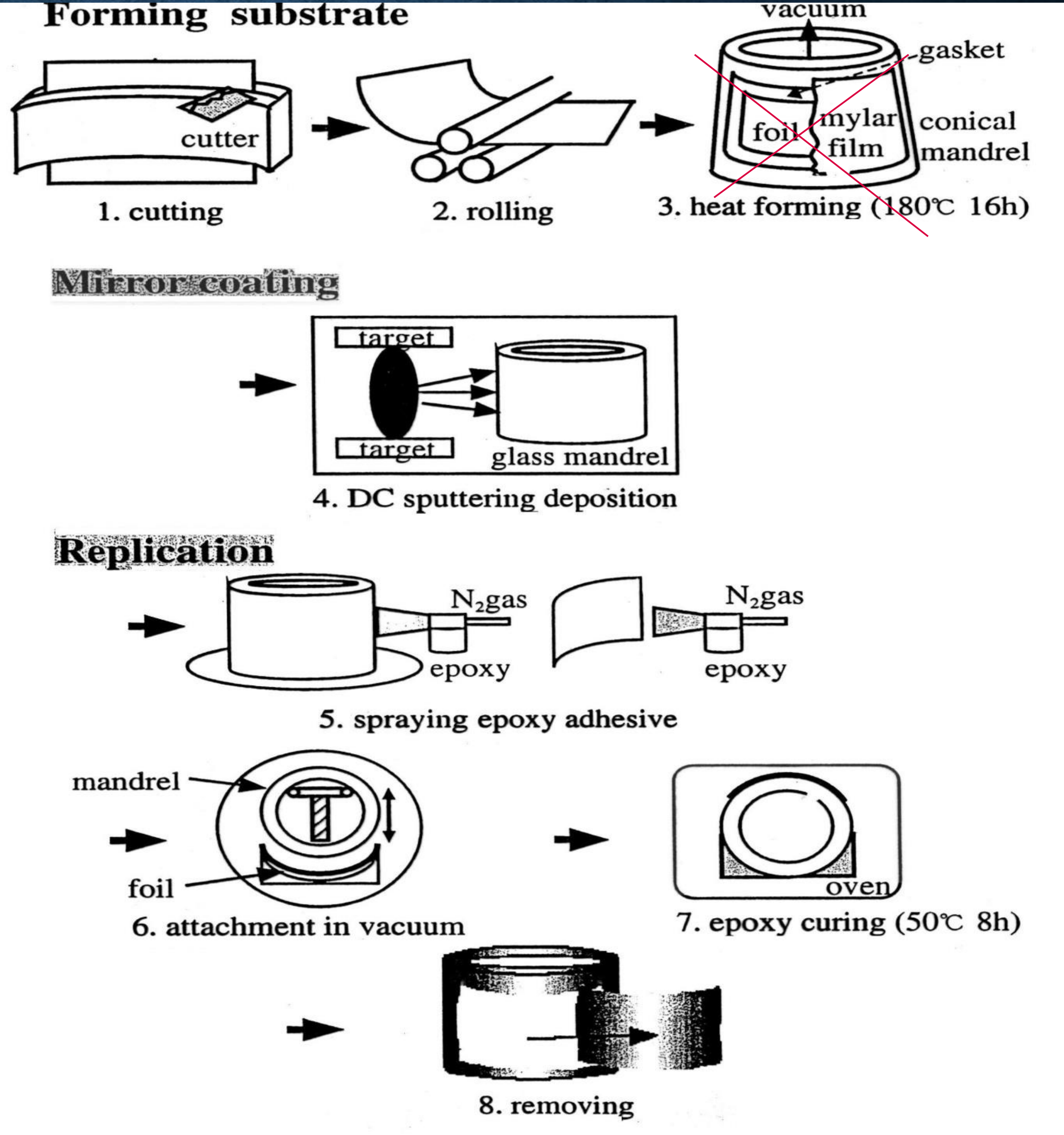

COMPARING TWO TYPES OF XRTS

Wolter-1 Optics vs.	Conical Approx. Optics
Exact machining of surface shapes	Approximate surfaces - easier to fabricate
Stiff and thick surfaces with low thermal expansion	Thin surfaces of metals (ready foils or replication)
Very poor nesting of many surfaces	Very high nesting possible
Small effective area	Larger effective area for same aperture
Limited high energy response or very large F.L. (8 - 10m)	Much better high energy response for same F.L.
Higher Angular resolution (arcsec)	Poorer angular resolution (arcmin)
Expensive Technology	Relatively much cheaper
Heavy (~ tonne)	Lighter (10 - 30 Kg.)
Einstein, ROSAT, Chandra	ASCA, Suzaku, AstroSat

Gold Surface Replication for AstroSat SXT

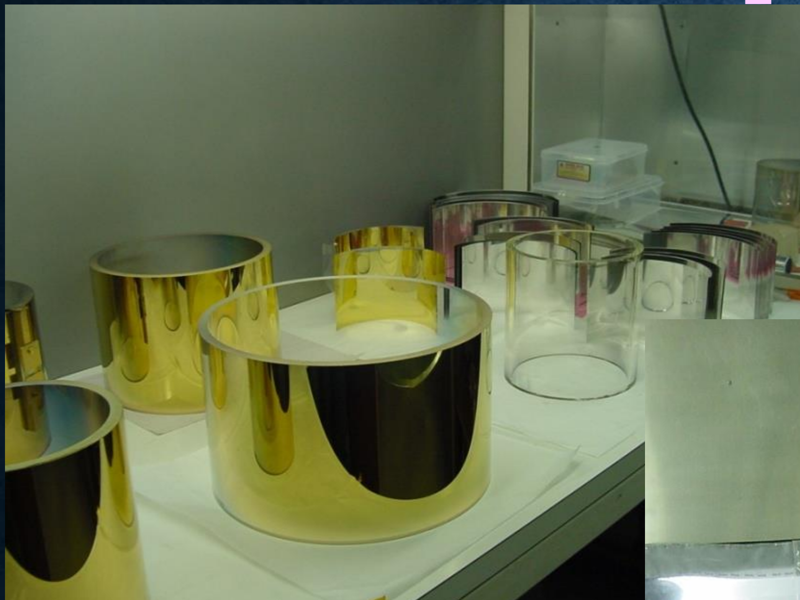

Gold Surface Replication: SXT

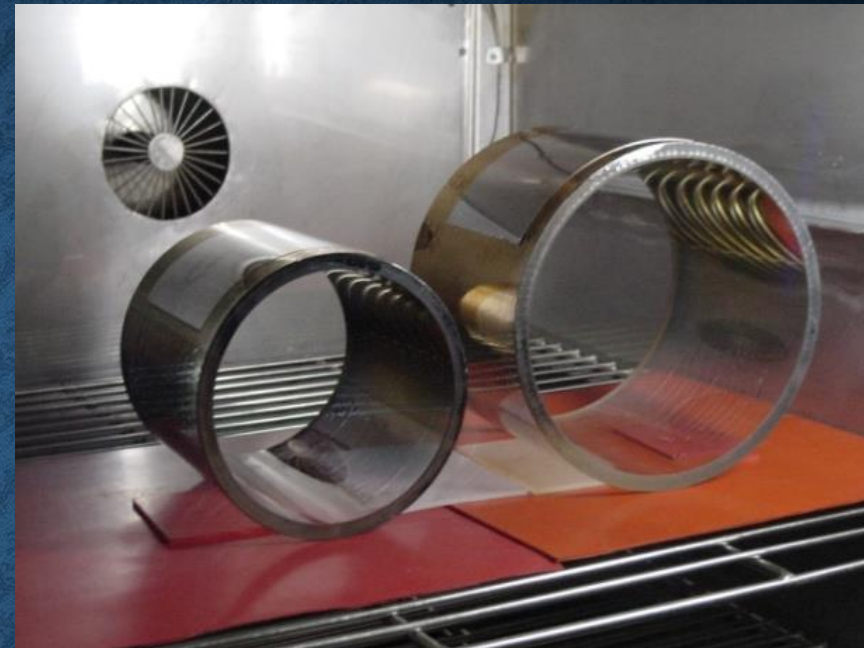

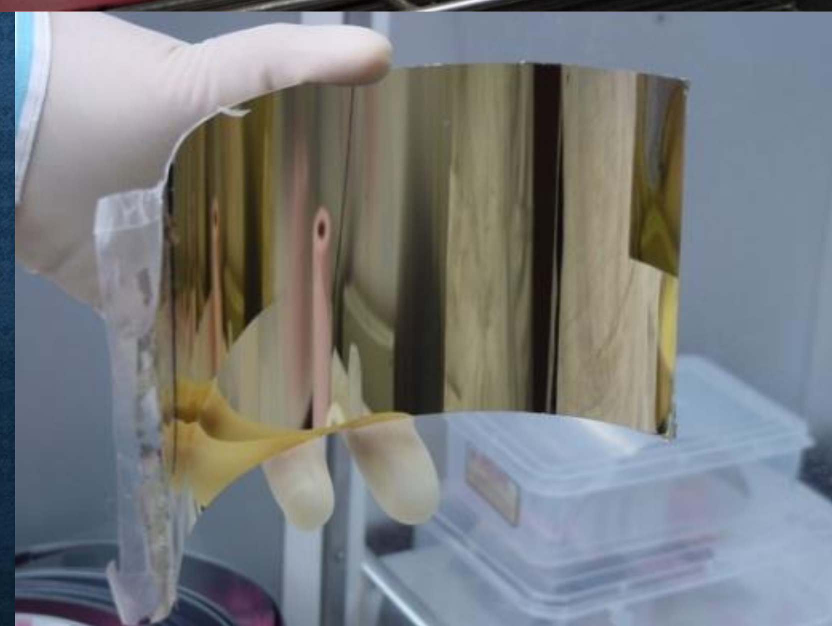

X-ray Ground calibration: SXT Mirrors

Performance of SXT grazing incidence foil mirrors evaluated using Indus-1 soft x-ray reflectivity beamline

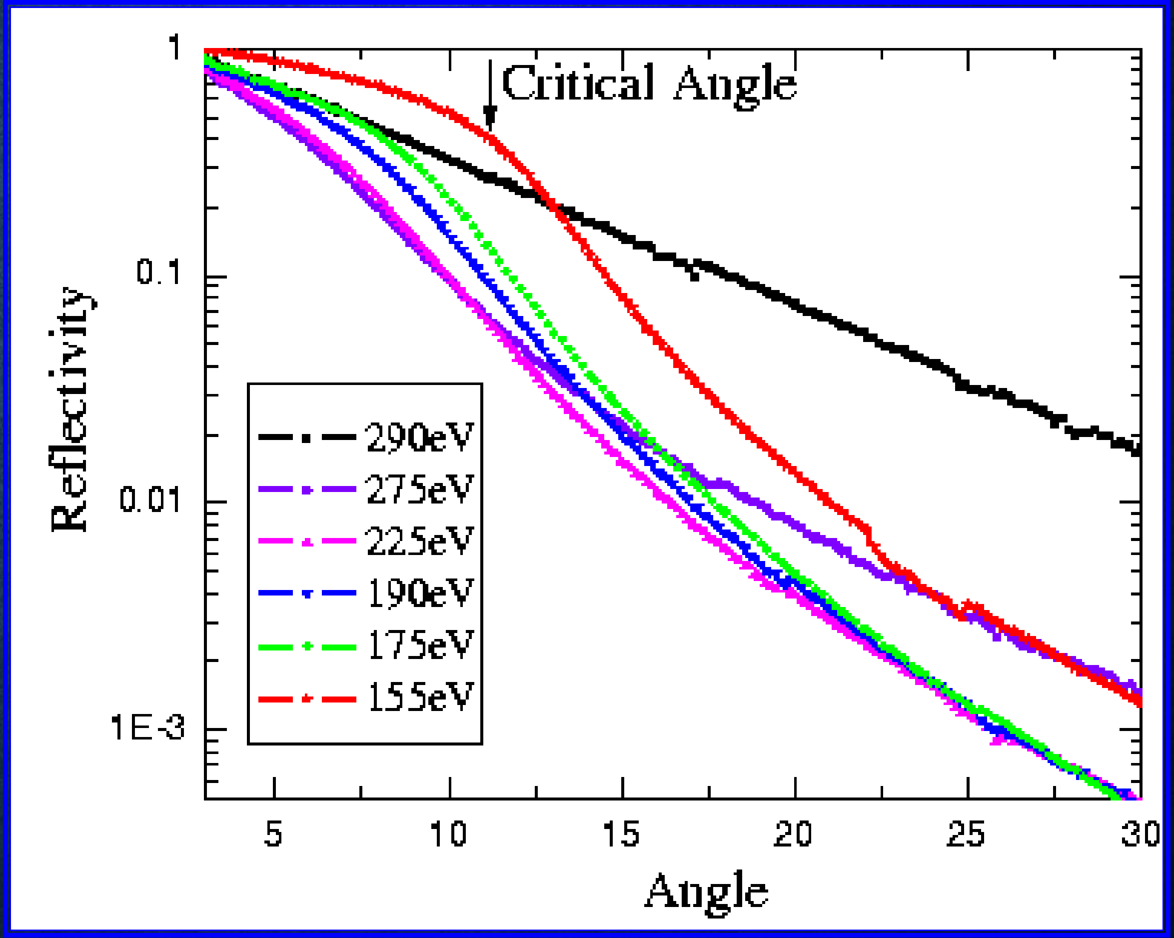

Archana et al Experimental Astronomy (2010)

X-ray Ground calibration

Performance of SXT grazing incidence foil mirrors evaluated at 5.4 and 8 keV.

Smoothness derived to be ~ 10 Angstroms

Surface layers are smoother than the deeper layers

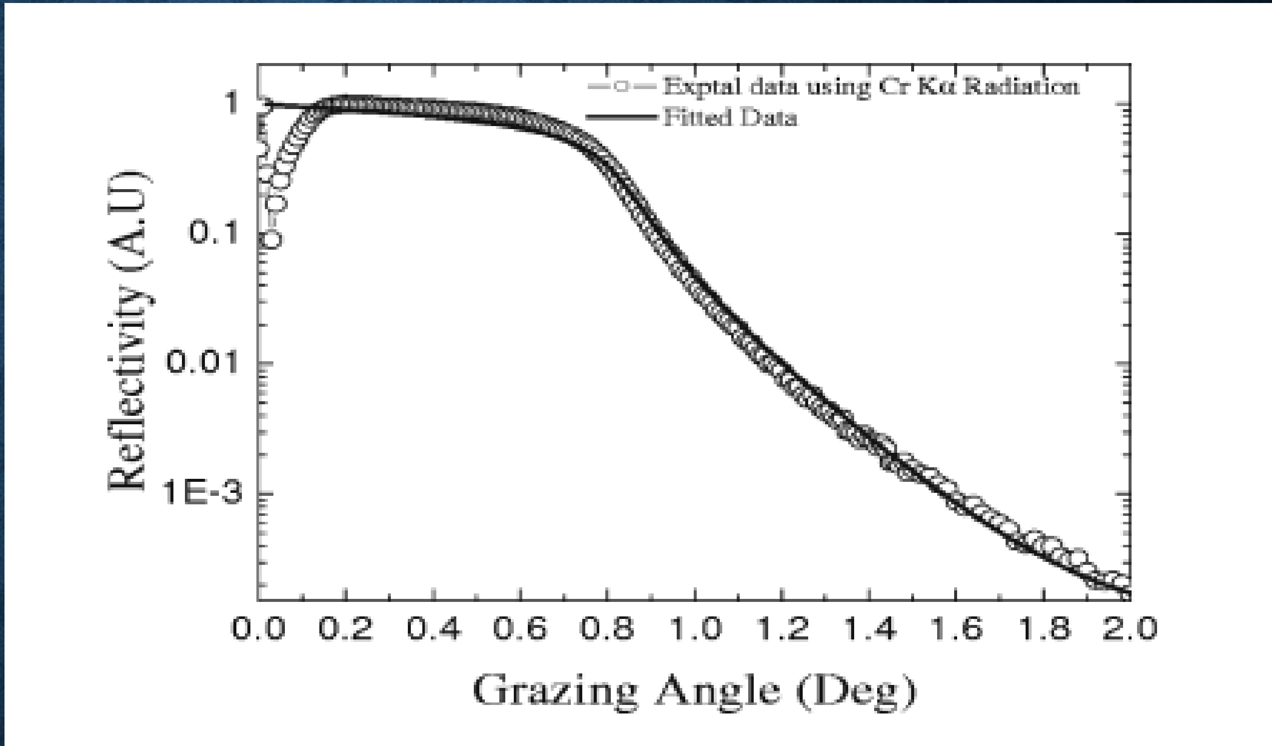

Fig. 6 X-ray reflectivity pattern obtained using Cr K_α X-rays for a typical sample of gold mirror

Archana et al Experimental Astronomy (2010)

ASTROSAT SXT: MIRRORS ASSEMBLY

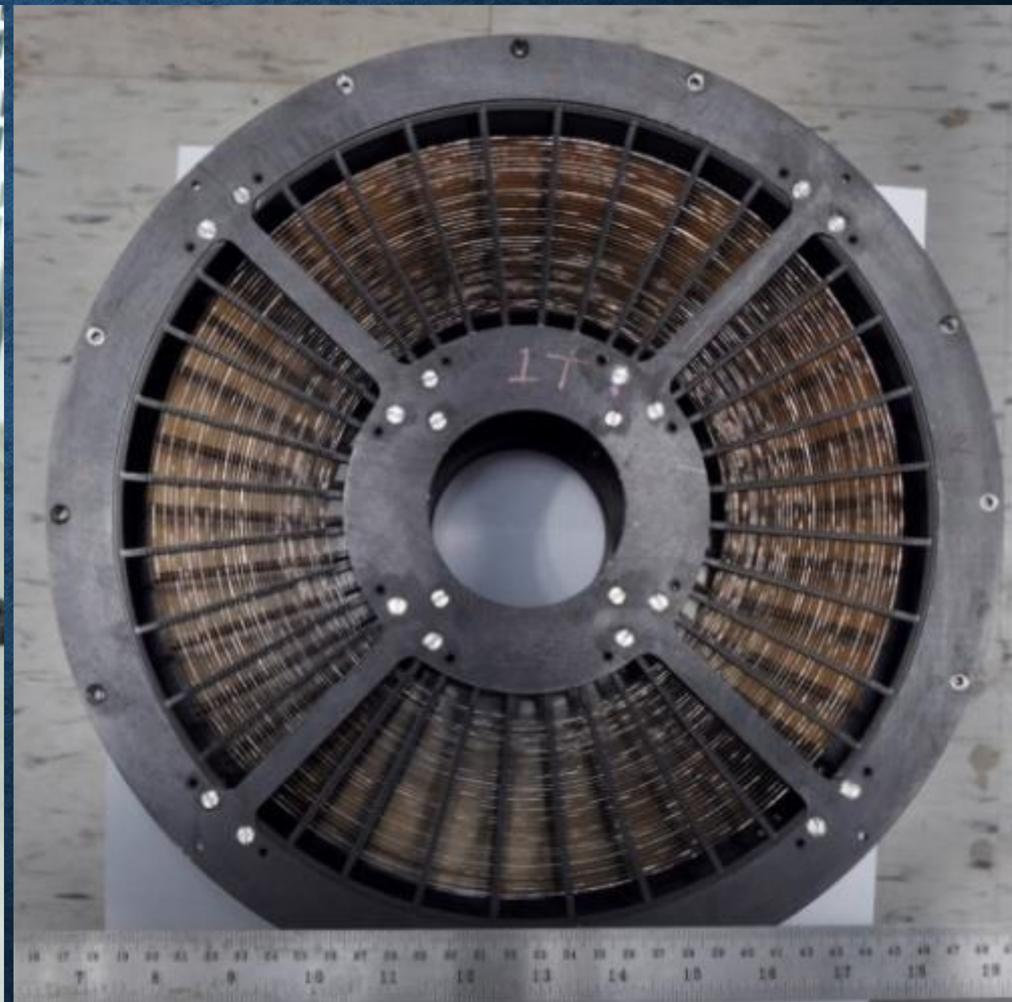

Number of nested shells = 40

SXT: OPTICS + CCD BASED FPCA(~65 KG)

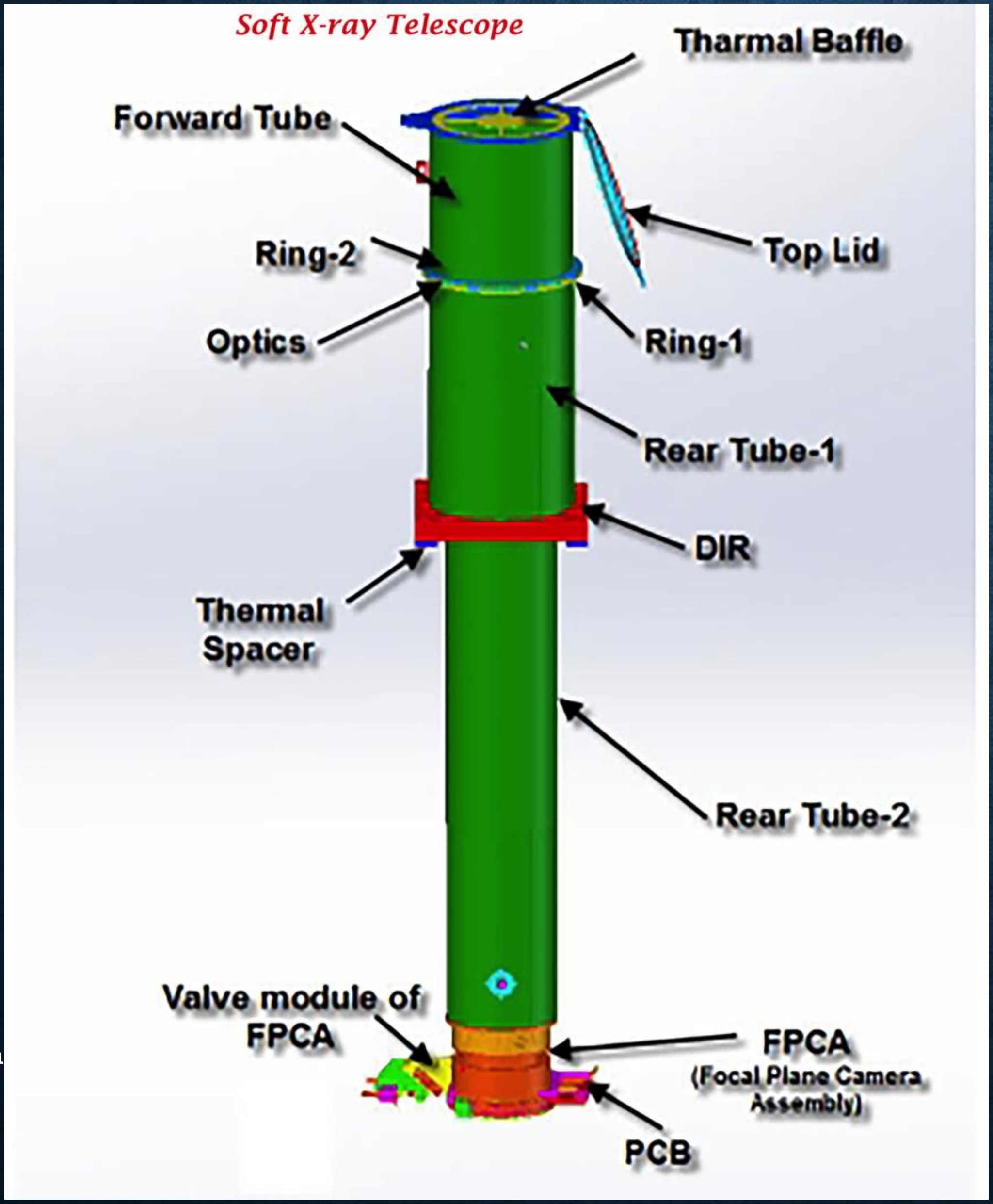

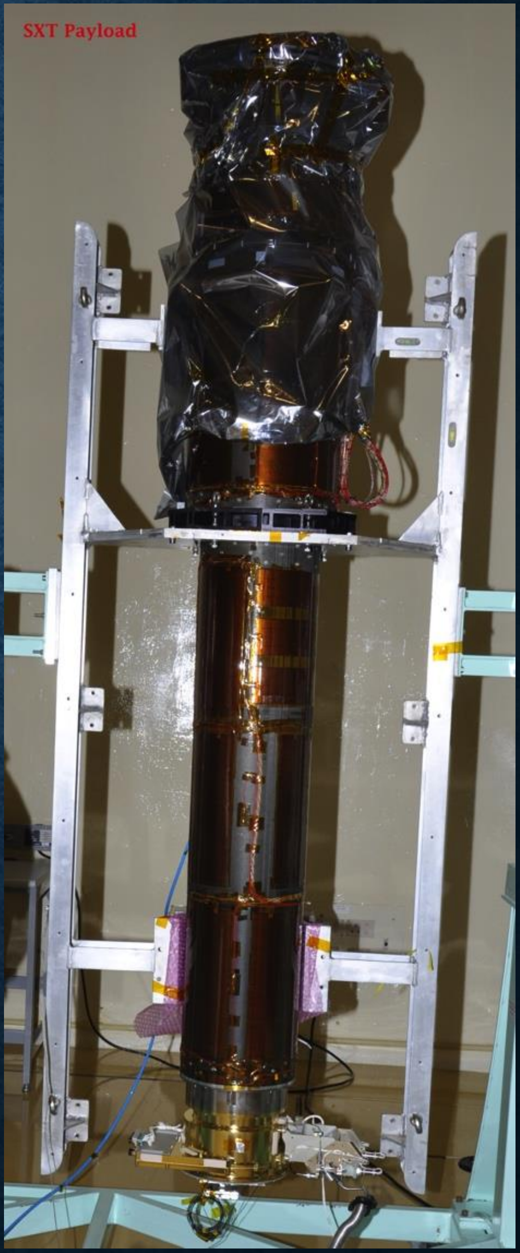

KPSin

SOFT X-RAY TELESCOPE

Telescope Length: 2460 mm
(Telescope + camera + baffle + door)
Top Envelope Diameter: 386 mm
Focal Length: 2000 mm
Maximum radius of foils: 130 mm
Minimum radius of foils: 65 mm

Reflector Length: 100 mm

Reflector thickness: 0.2 mm (Al) + Epoxy (50-60 microns) + gold 1400 Angstroms

Minimum reflector spacing: 0.5 mm

No. of reflectors: 320

ASTROSAT SXT: FM

- Characterization and proof of assembly thru Optical laser beam tests of all individual mirrors (320) and full beam. Depth of focus checked – no change up to 3-4 mm

Full aperture optical light test to check the FM SXT optics at 2m focal length

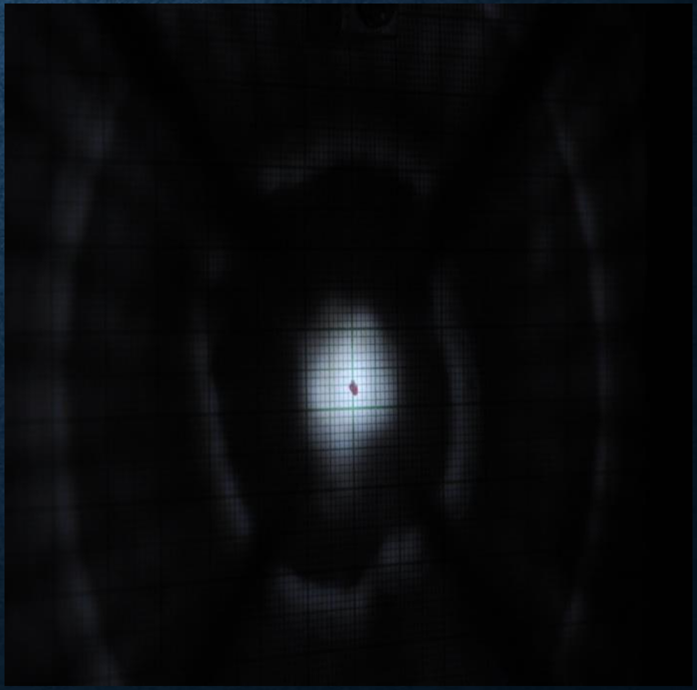

Angular Resolution (Half-power diameter) = ~3-4 arcmin

Field of View (1 CCD) = 41 x 41 arcmin

KPSingh

SXT- Focal Plane Camera Assy

Modified from Swift; Using spare MOS CCD22 from XMM: 600 x 600 pix, 40 microns

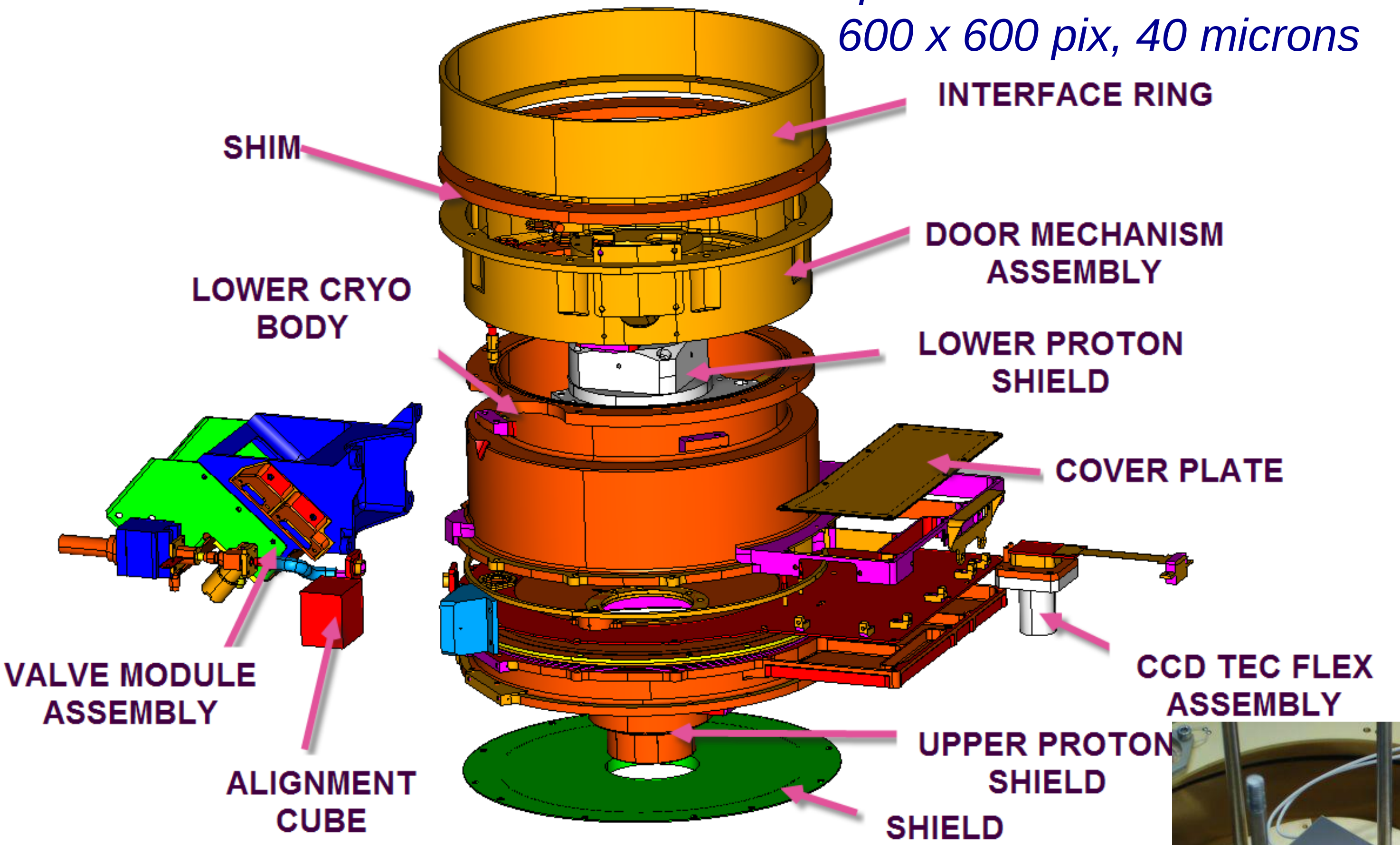

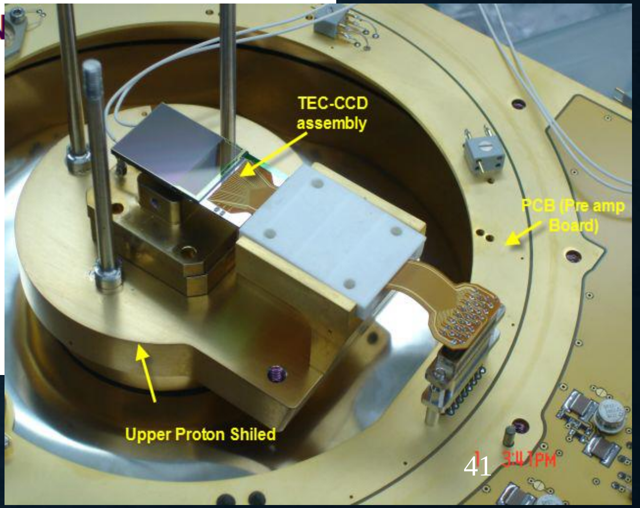

- Four Fe-55 calibration (corner) sources
- One Fe 55 calibration door source
- Thin Optical Blocking Filter
- CCD Assy. including TEC
- PCB with front-end electronics

SXT : Area, Resolution, Sensitivity

- Effective area
  - ~75 cm^2 at 1.5keV
  - Sensitivity : 10^{-13} ergs cm^{-2} s^{-1} (5-sigma detection in about 25ks)
- Energy resolution
- 90eV@1.5keV, 136eV@5.9keV
- Moderate Time resolution
  - PC mode : ~2.4 s
  - FW mode : ~0.278 s
- Soft X-ray spectroscopy for sources with **2-10 keV flux > $3x10^{-12}$ ergs cm^{-2} s^{-1}**

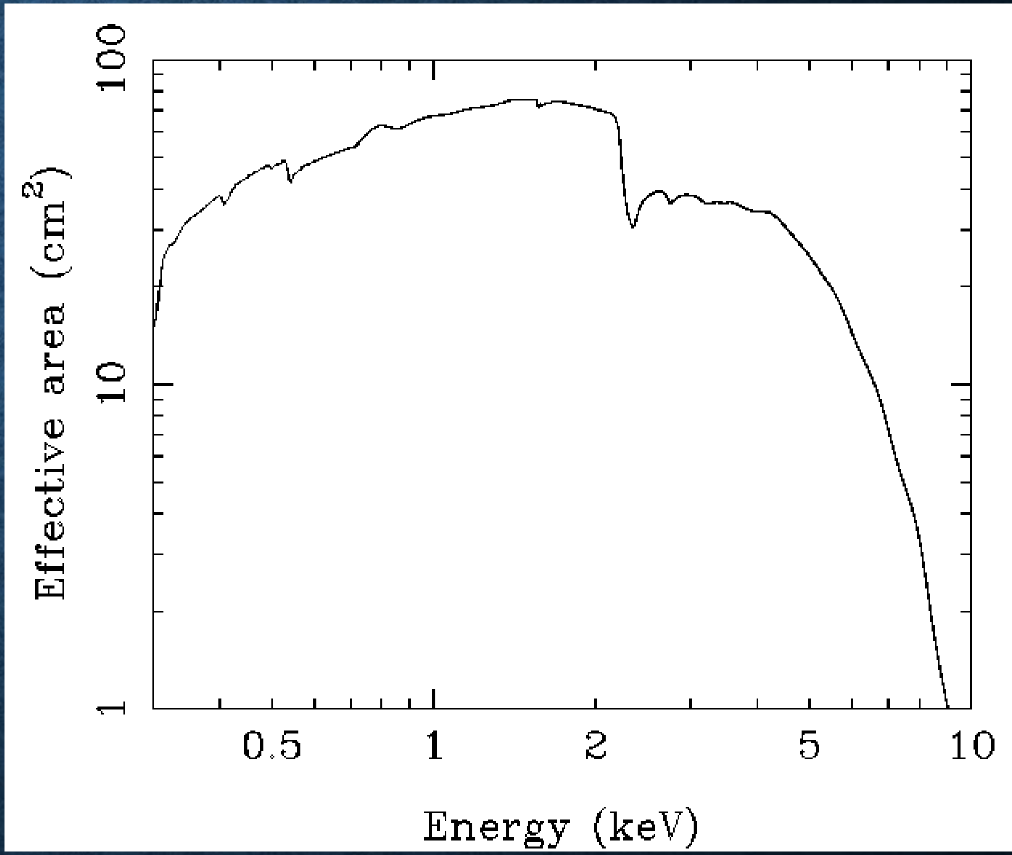

AstroSat in a clean room before Launch

SXT: India's first Soft X-ray Imaging Telescope

Mass of 1513 kg. (750 kg. Payloads)

SXT CCD – Calibration sources and the filter image

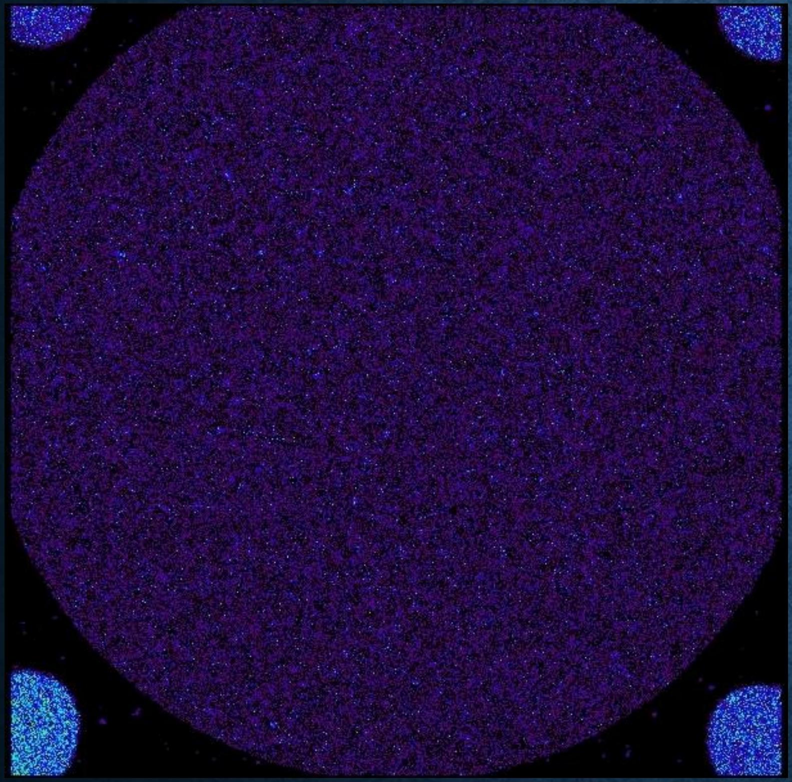

Door and Corner X-ray Calibration Sources

CCD: 600x600 pixels; 40 micron each

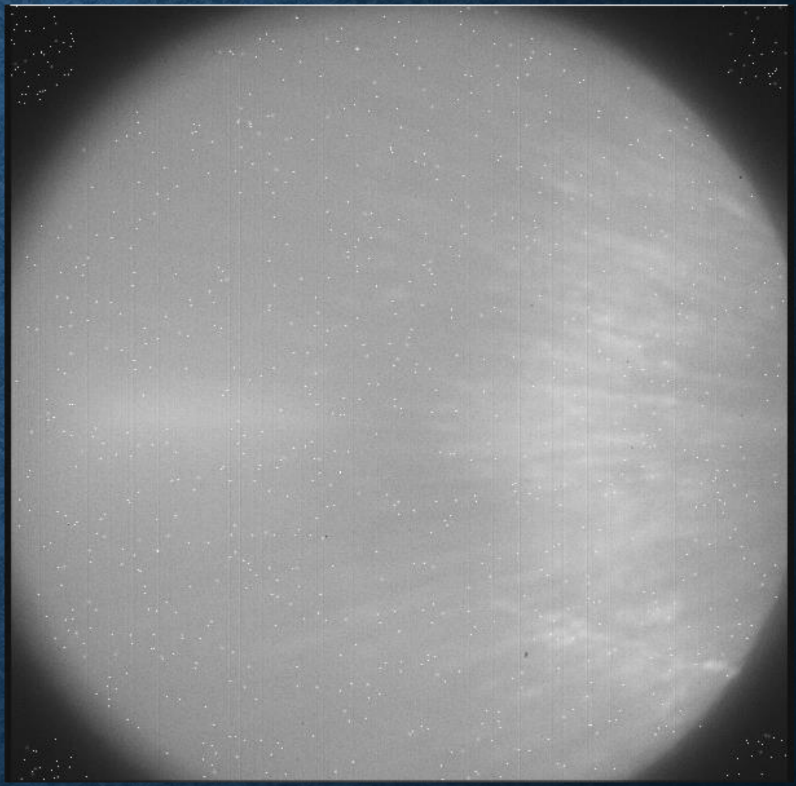

Optical LED Image of the filter

SXT SWITCH ON AND FIRST LIGHT

- Telescope (Optics) Door opening - Oct 15th
- Camera Door Opening - Oct 26th @ 06:30 UT
- First Light – Oct 26th

Pointed at and observed- PKS2155-304 (Quasar) at redshift of 0.116

(1.6 Billion LY away)

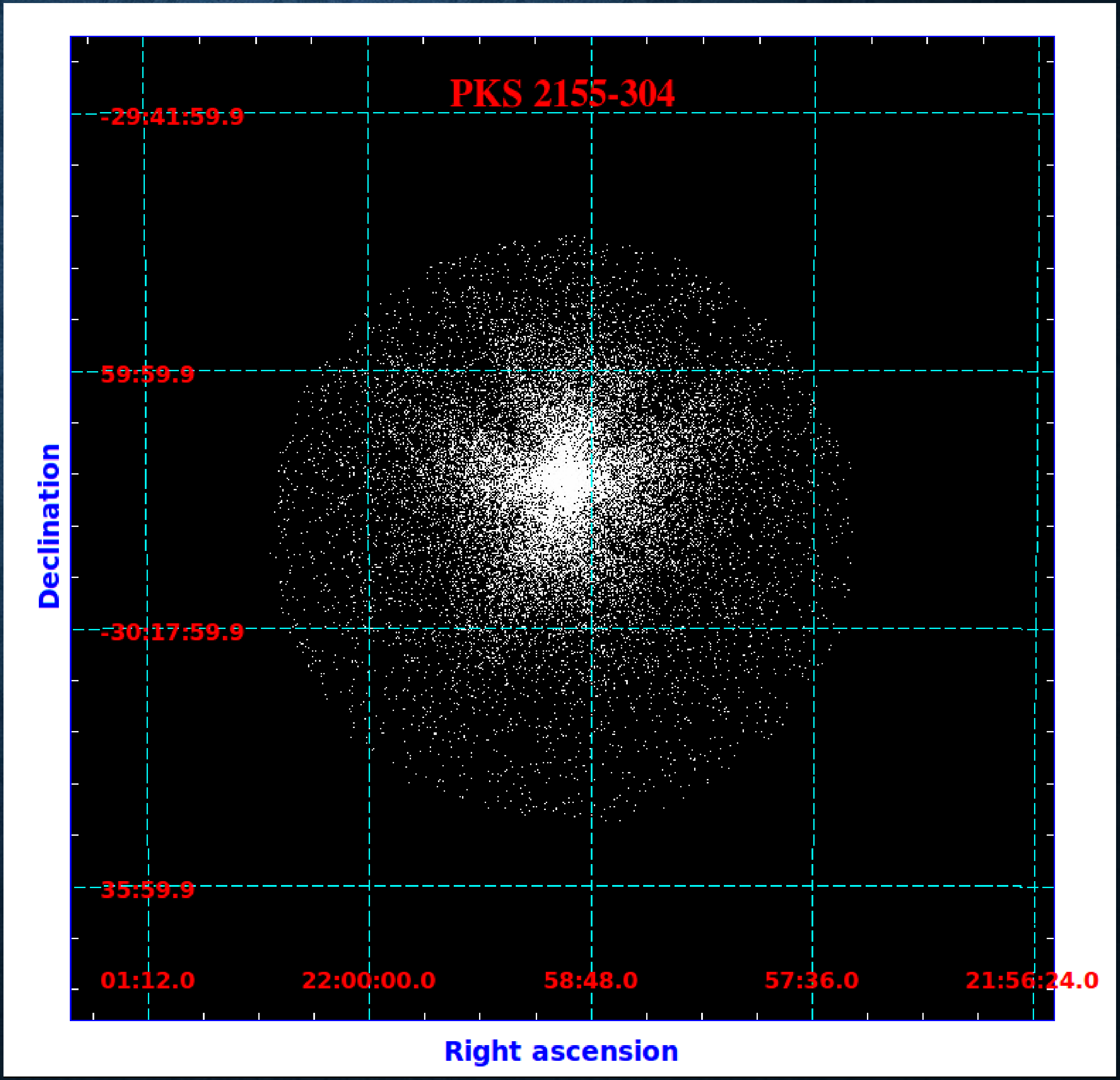

PKS 2155-304: BORE SIGHT, CALIBRATION

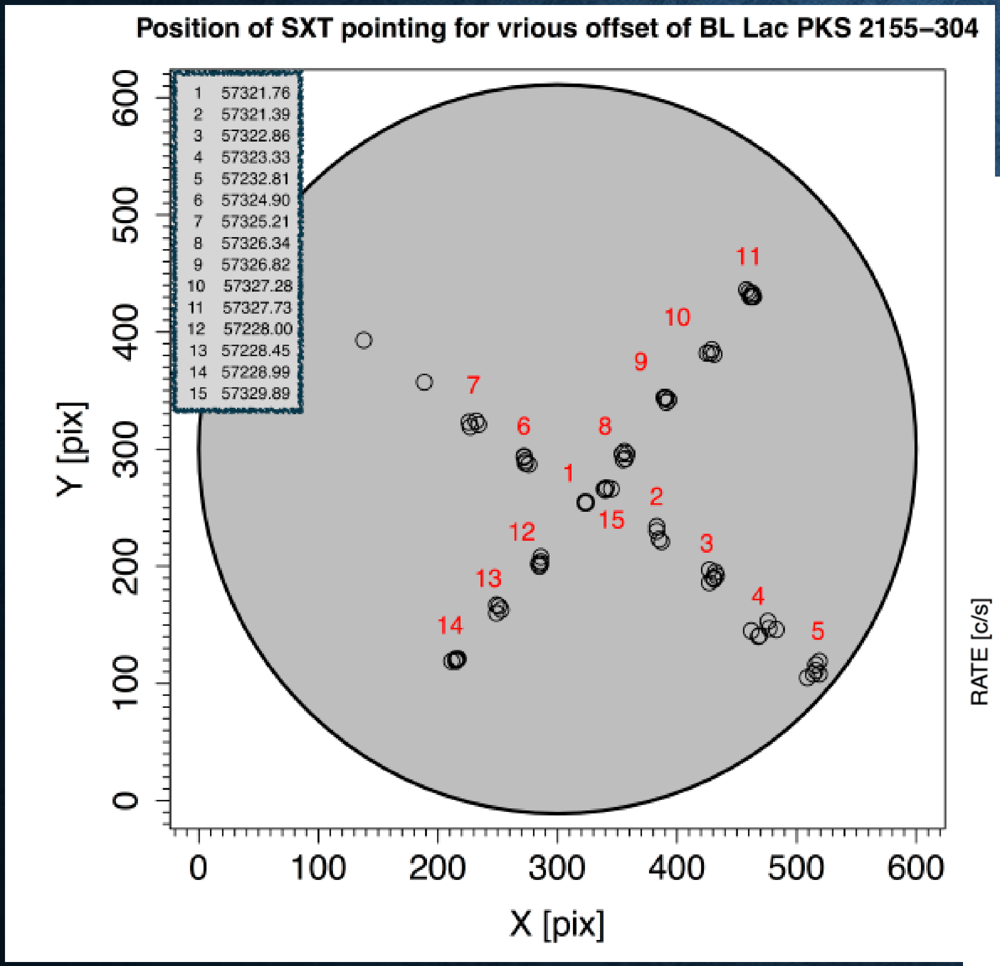

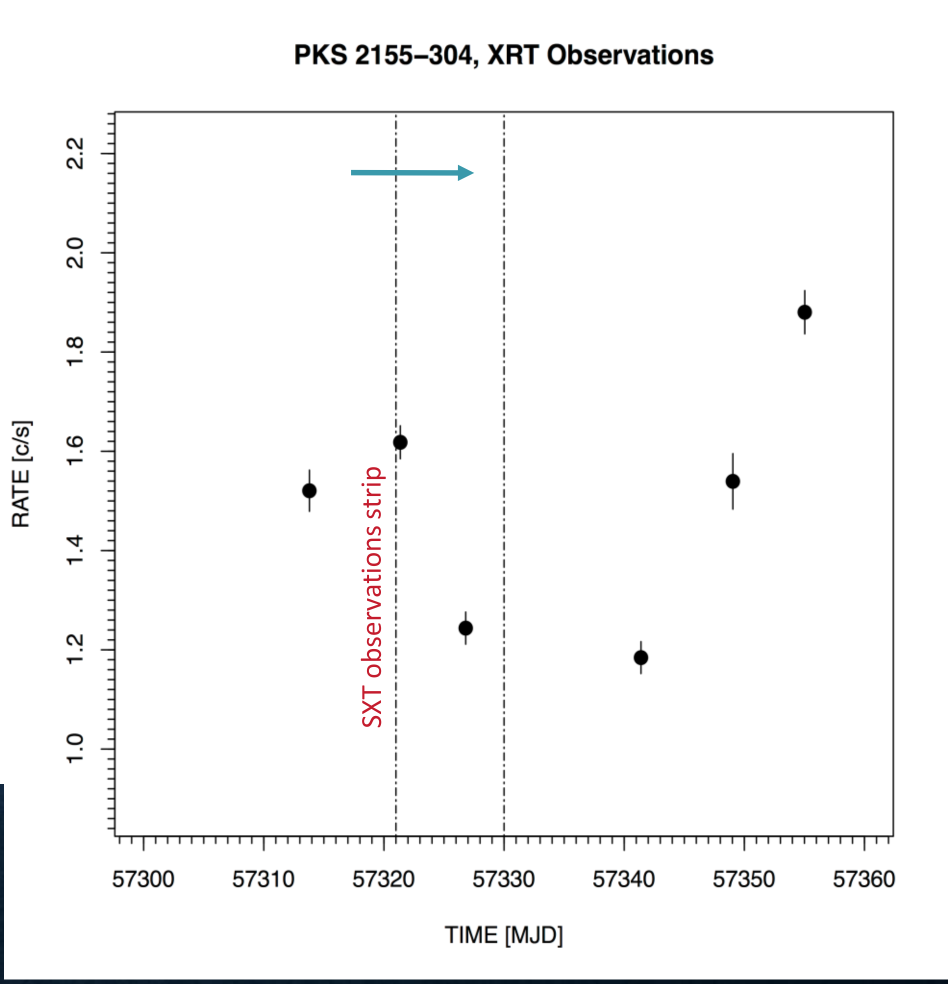

K.P.Singh

SXT Performance : Imaging

- PSF : 2' (FWHM), 10' HPD

Advantage : No pile-up for bright sources < 200 mCrab

Disadvantage: NO area in the detector for simultaneous background measurement

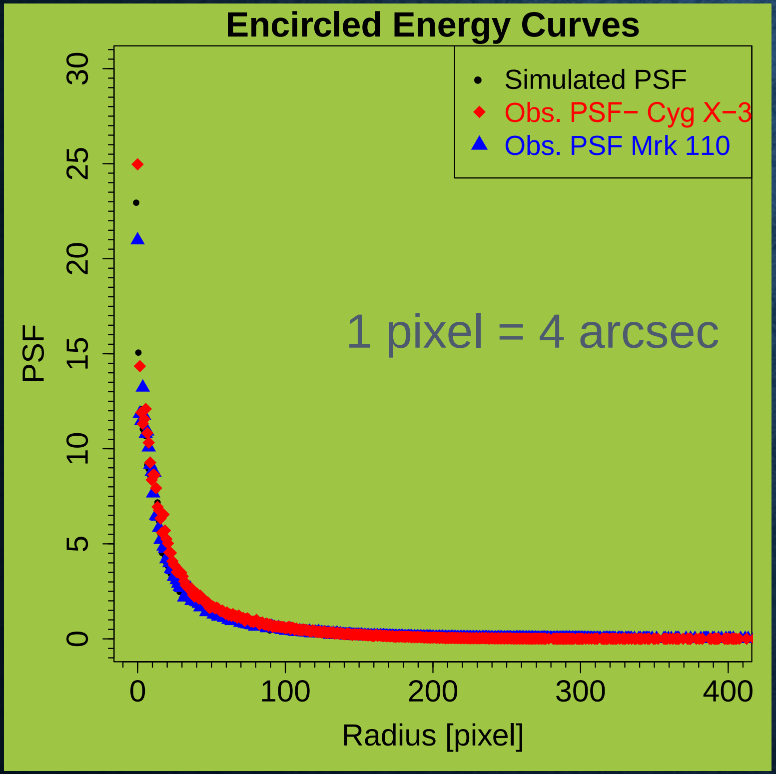

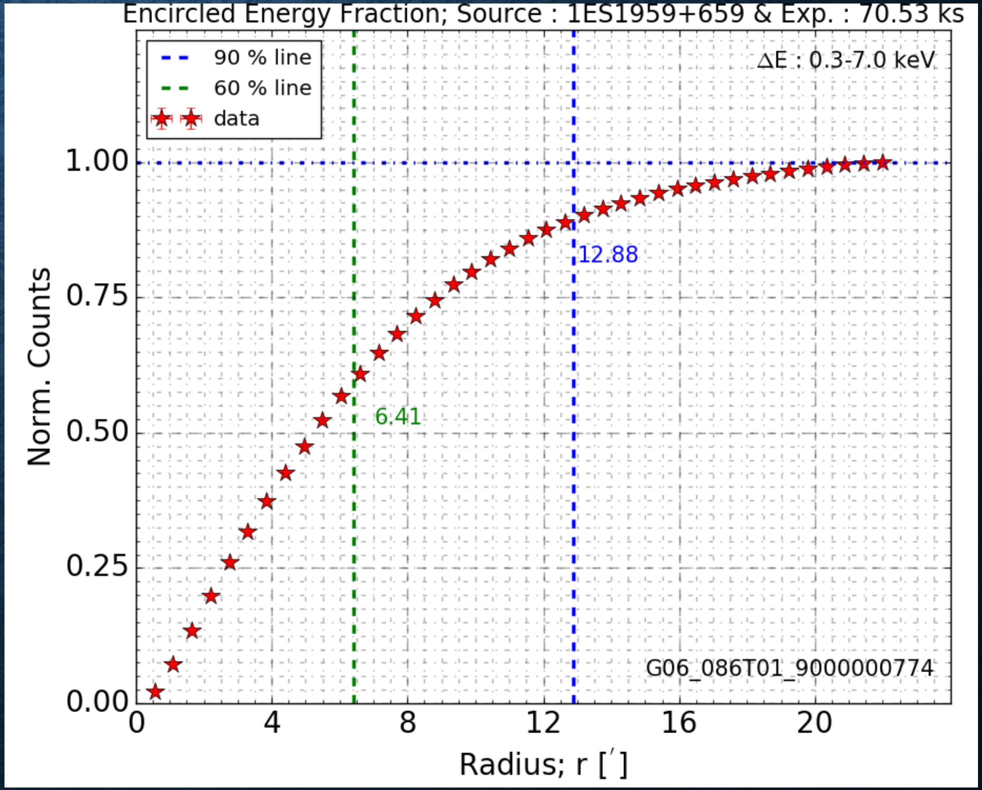

No significant energy or offset dependence

K.P.Singh

Vignetting function Using SNR 2E0102-7217

$$V(\theta) = 1 - C\theta^2$$

θ is the off-axis angle, and the coefficient C is a function of energy (in keV),

$$C(E) = P_0 \times P_1^{E} + P_2$$

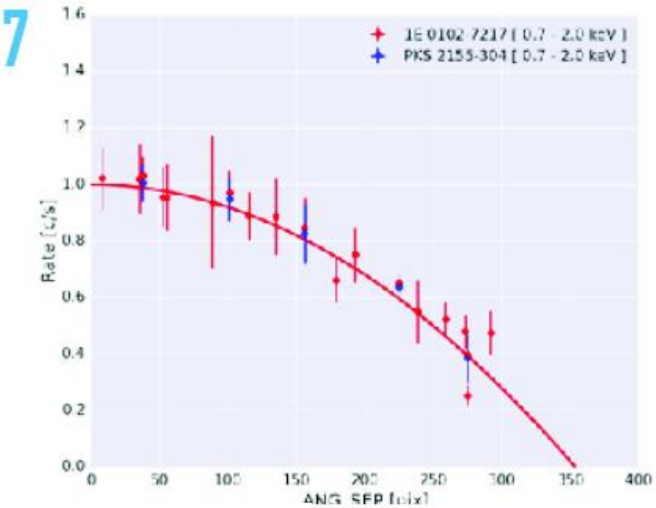

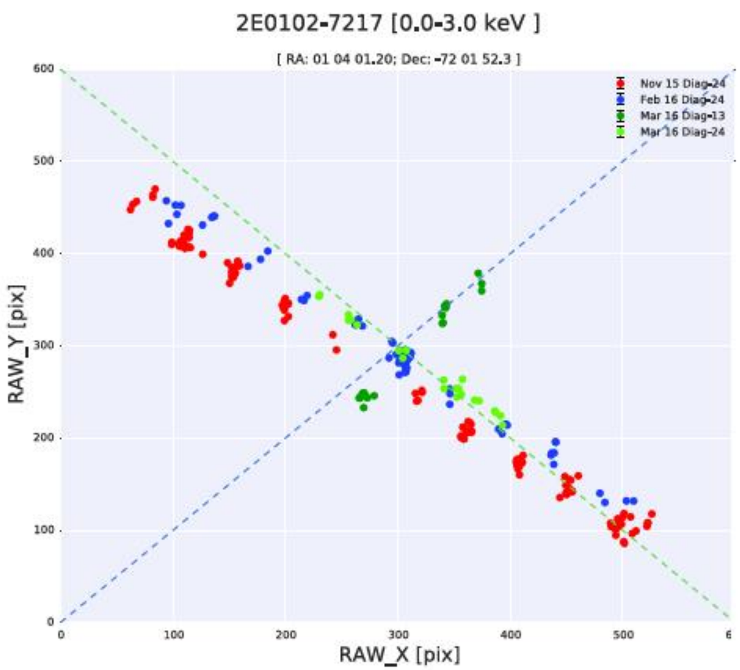

P_0 = -2.492e-06
P_1 = 0.9996
P_2 = 9.6120e-06

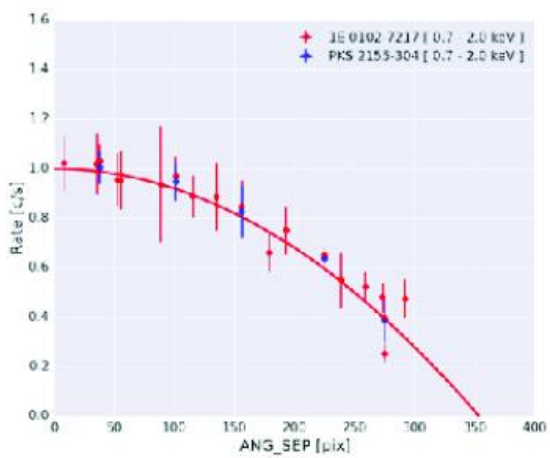

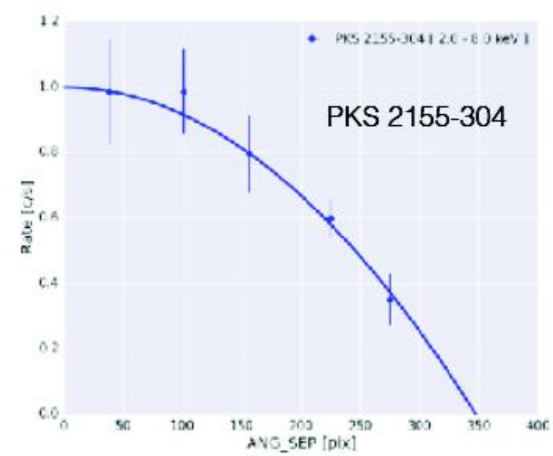

Singh et al. 2017, (Telescope Description and Calibration Status), In preparation

SXT Performence : Vignetting function

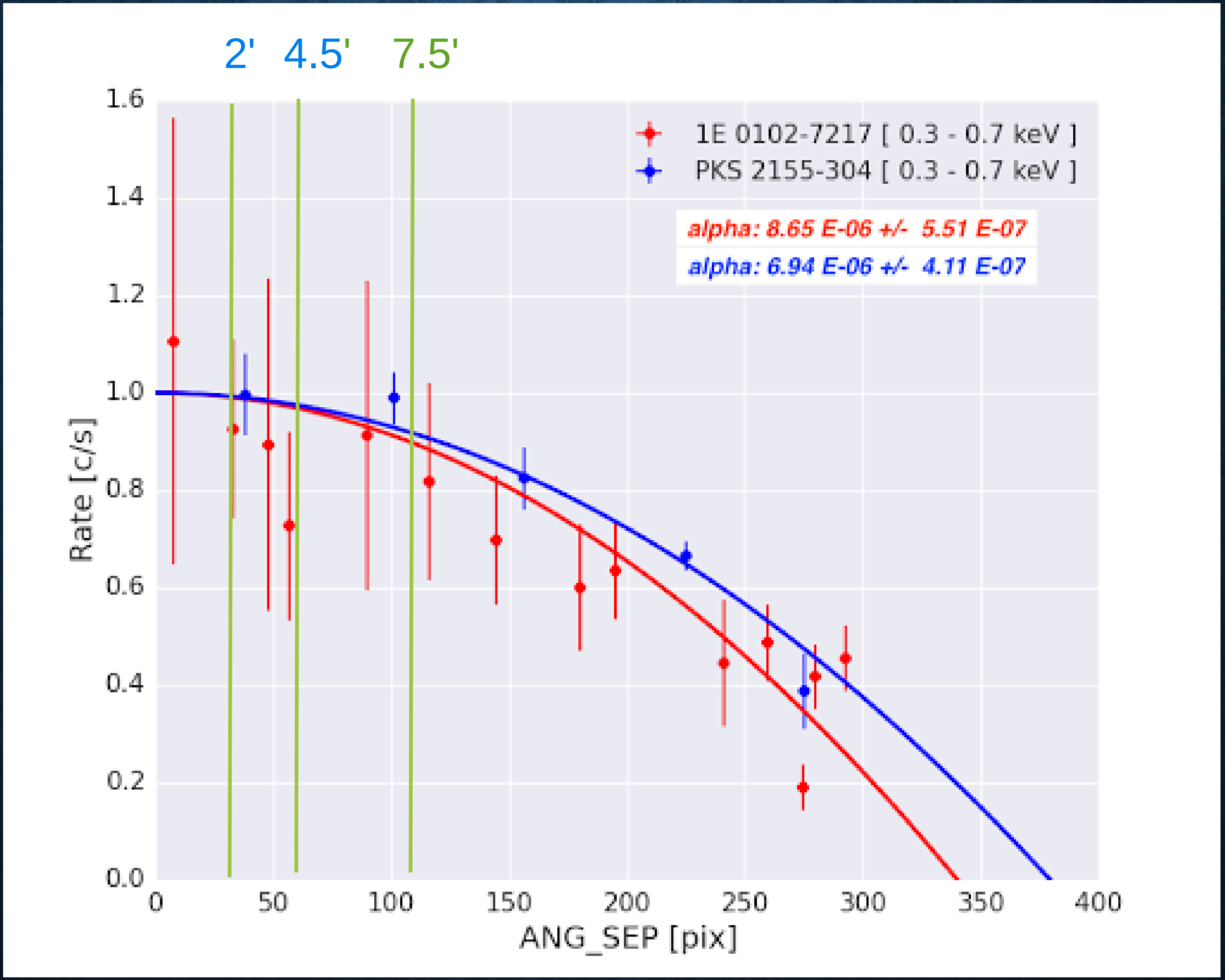

SXT Performance : Spectral Response

- ARF: recalibrated using Crab observations (Feb 2017), Issues at low energy < 0.5keV
- RMF : gain change ~ 20-40eV, issues at low energies, Above 0.5 keV okay with a few % systematic error (ARF/RMF need further corrections!)
- Background : Low and steady background, average background spectrum from blank sky observation available.

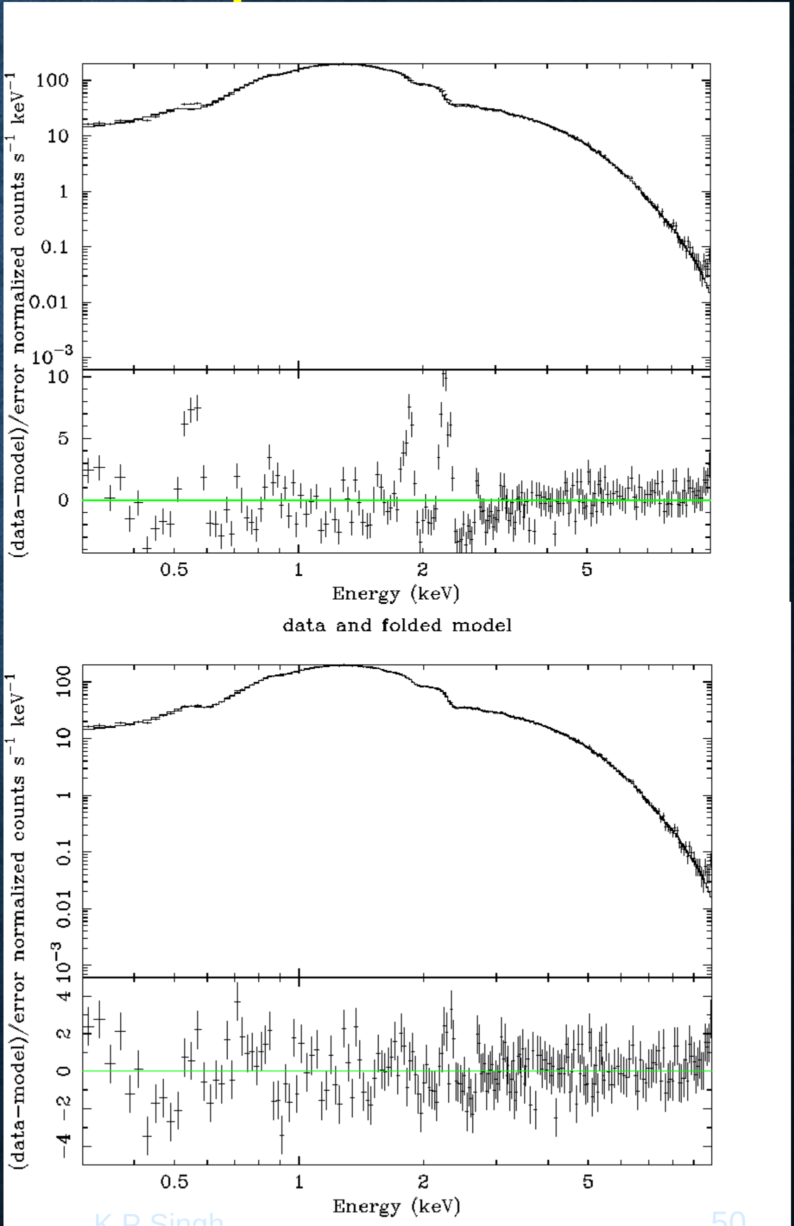

2E01020-72: *Spectral Fit using the IACHEC Model*

IACHEC Model: Plucinsky et al. 2016

The very soft band of the SXT

Credits:
S. Chandra
+ SXT team

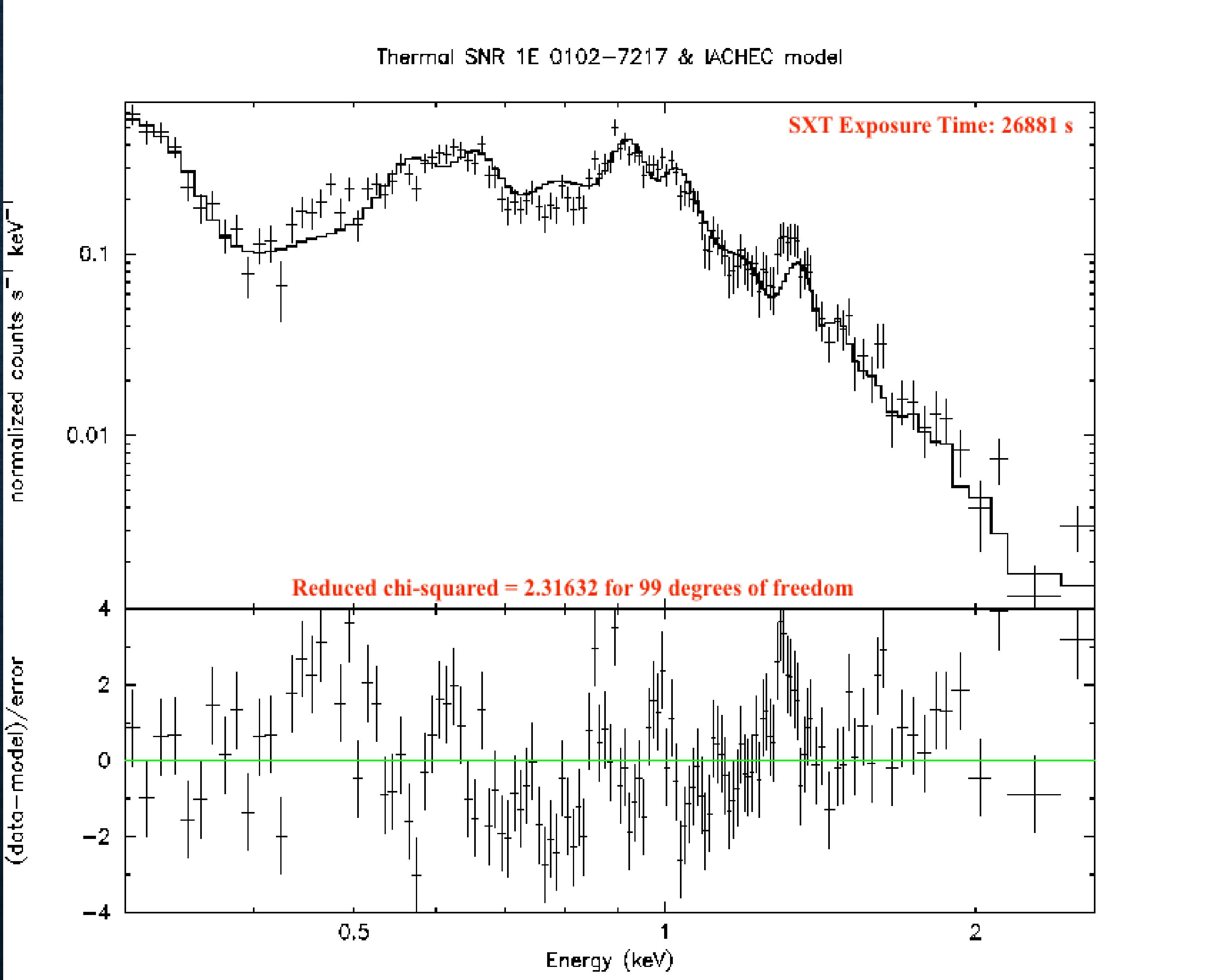

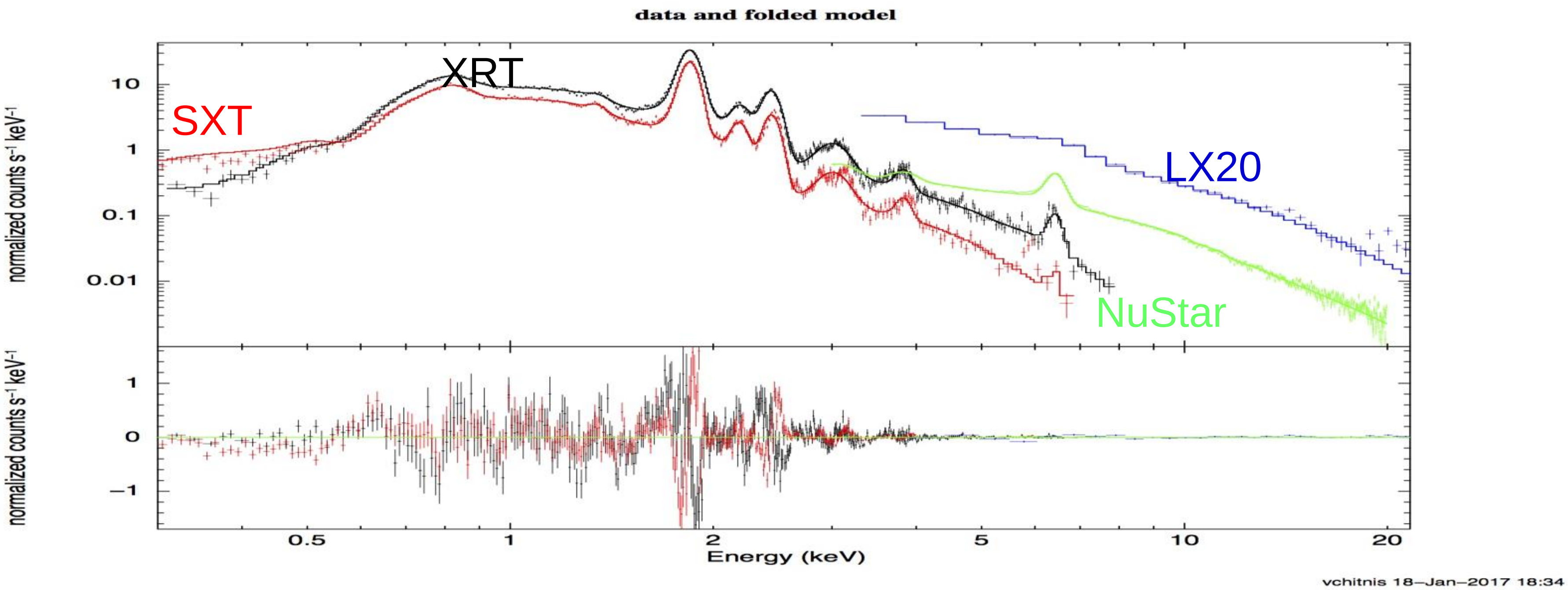
data and folded model
XRT
SXT
LX20
NuStar
normalized counts s^{-1} keV^{-1}
Energy (keV)
vchitnis 18–Jan–2017 18:34

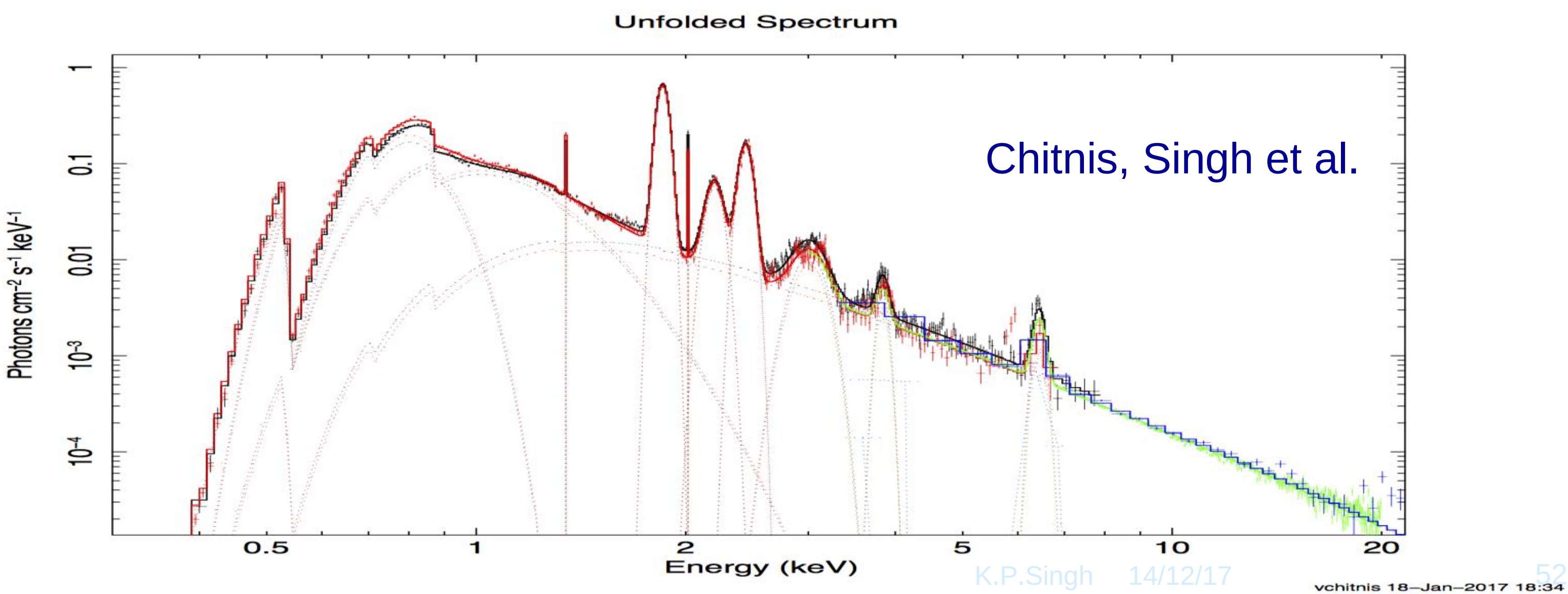
Unfolded Spectrum
Chitnis, Singh et al.
Photons cm^{-2} s^{-1} keV^{-1}
Energy (keV)
vchitnis 18–Jan–2017 18:34

ANALYZING SXT DATA: READOUT MODES OF THE CCD

(1)Photon Counting Mode (PC), [Full foV: The Default Mode - includes the calibration sources]

(2)Photon Counting Window Mode (PCW) – 5 pre-defined windows recommended.

(3)Fast/Timing Mode (FM): reads only the central 150 x 150 pixels (10x 10 arcmin) of the CCD. For observing very strong cosmic sources like Crab, Cyg X-1 etc.

(4)Bias Map Mode (BM), and

(5)Calibration Mode (CM): where four small windows (each of size=80 x 80 pixels) covering only the corners are used for the corner radioactive sources in the CM. (A central 100x100 window is also used in the CM).

- X-ray spectral information available in all the modes.
- Time resolution in the PC, PCW, CM modes is 2.4 s, and 0.278 s in the FM mode.

- Energy threshold applied only in PC, FW, PCW modes.

SXT: Analyzing Data

Level 1 SXT data from *each orbit* are run through the SXT pipeline at the SXT POC, and filtered for Bright Earth Avoidance, SAA, and events grades 0 to 12 only are accepted → Level2 orbit wise data – cleaned events, image. Light curve and spectra from the entire CCD frame.

A Julia/python tool is provided to merge Level2 data and remove all overlap of “gti’s” etc. create a single merged “events” file.

The merged events file can be read by “XSELECT” and final images, light curves and spectra can be created by the user.

The telescope area efficiency, detector response function and a deep background spectral and events file are provided to the user for further analysis

All products created using XSELECT are compatible with the HEASOFT pakage.

NGC 4151:
SXT AND LAXPC - A COMPARISON OF BACKGROUNDS

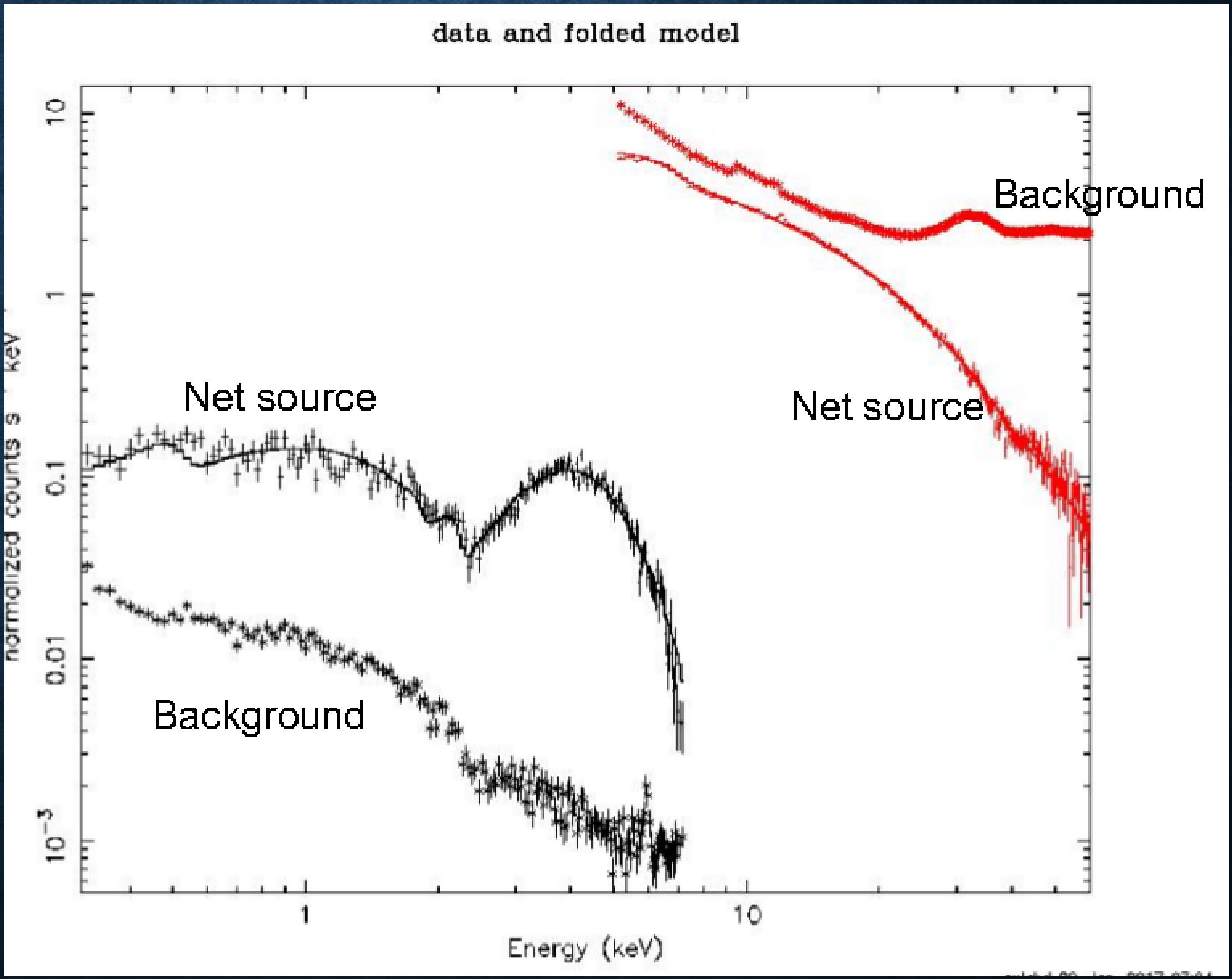

Mar 14-16, 2016: PV data

NGC4151: SXT+LAXPC SPECTRUM OVER A WIDE X-RAY BAND

Absorbed PL (0.3-5keV, 7-10, 40-60keV)

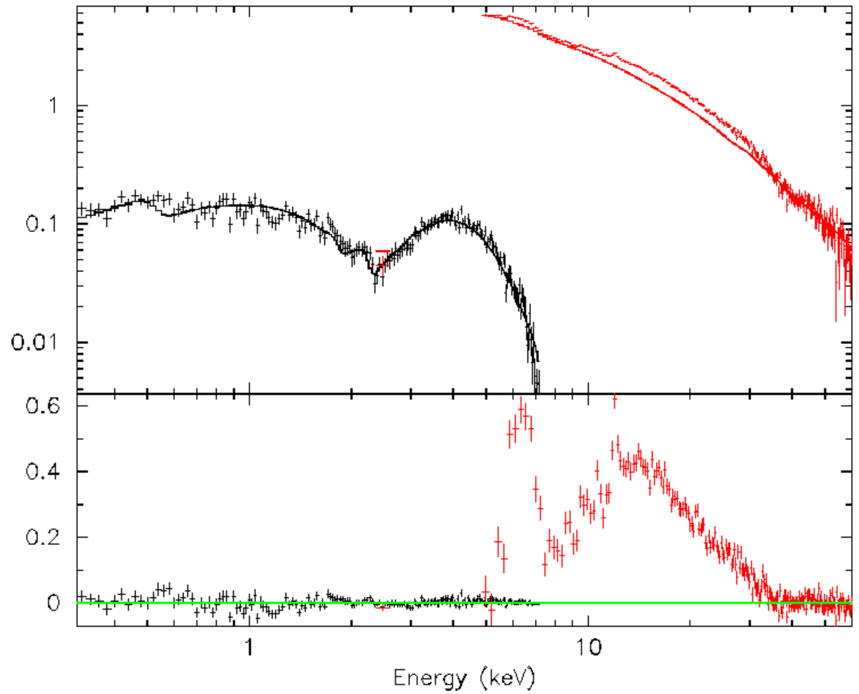

pcfabs*(pexrav + gauss)

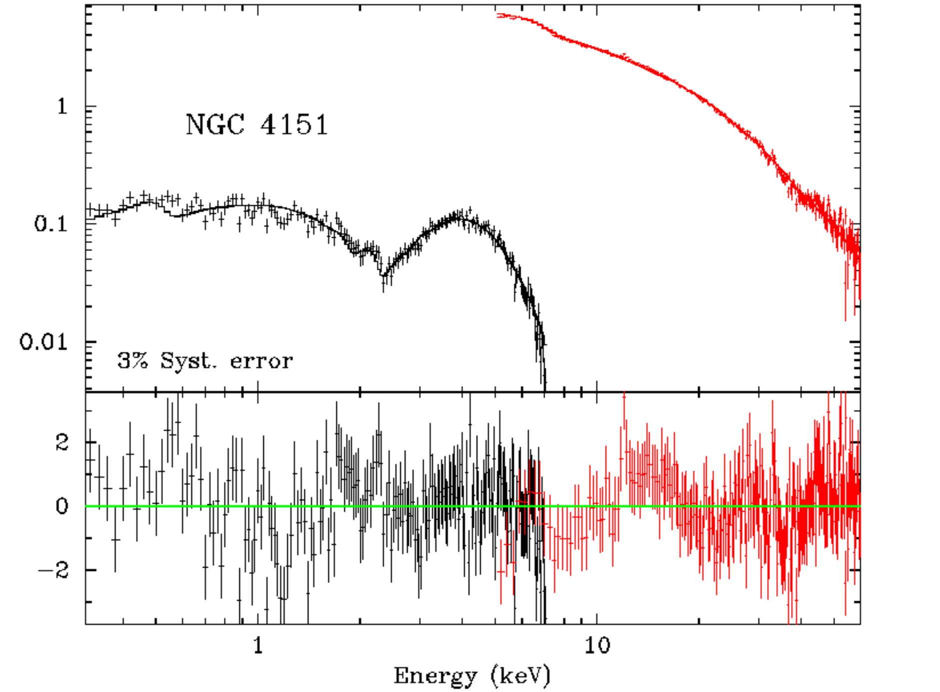

Reduced chi^2 = 1.3

NGC 4151 : z=0.00326
SXT & LAXPC CROSS-CORRELATION

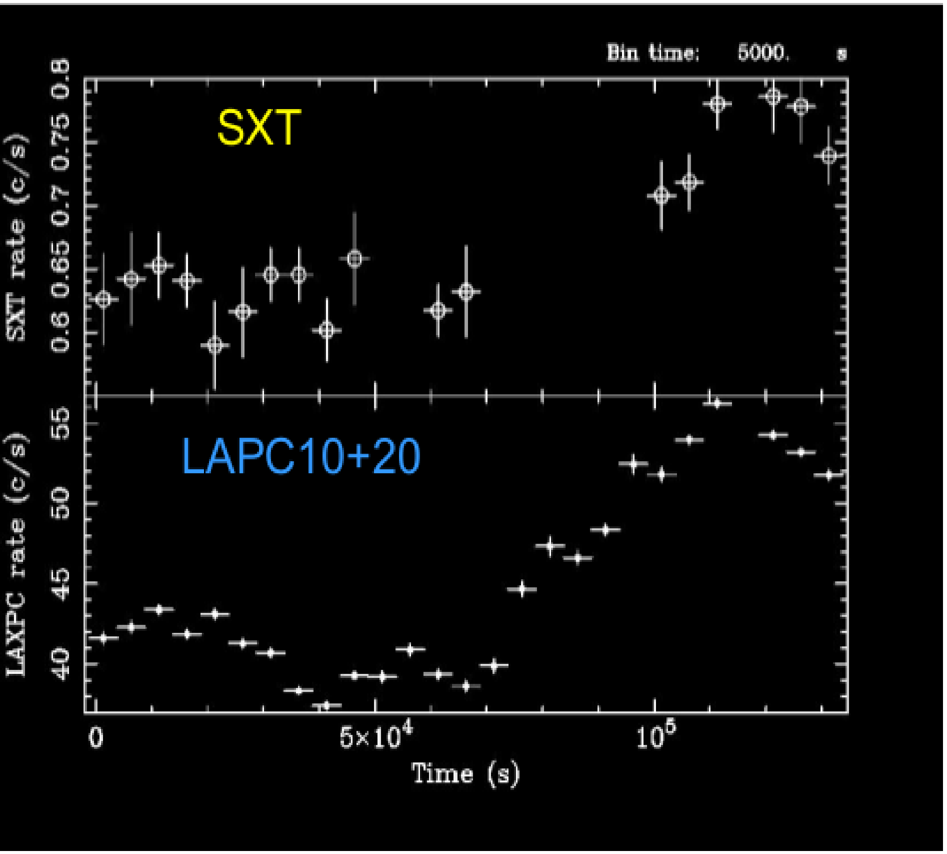

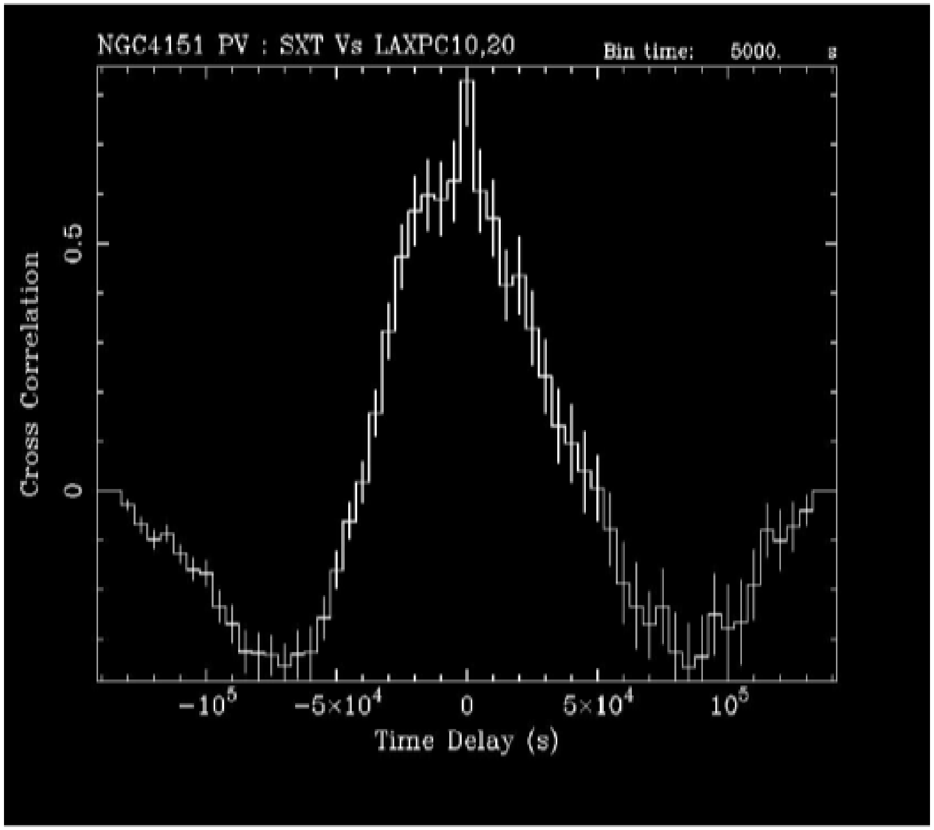

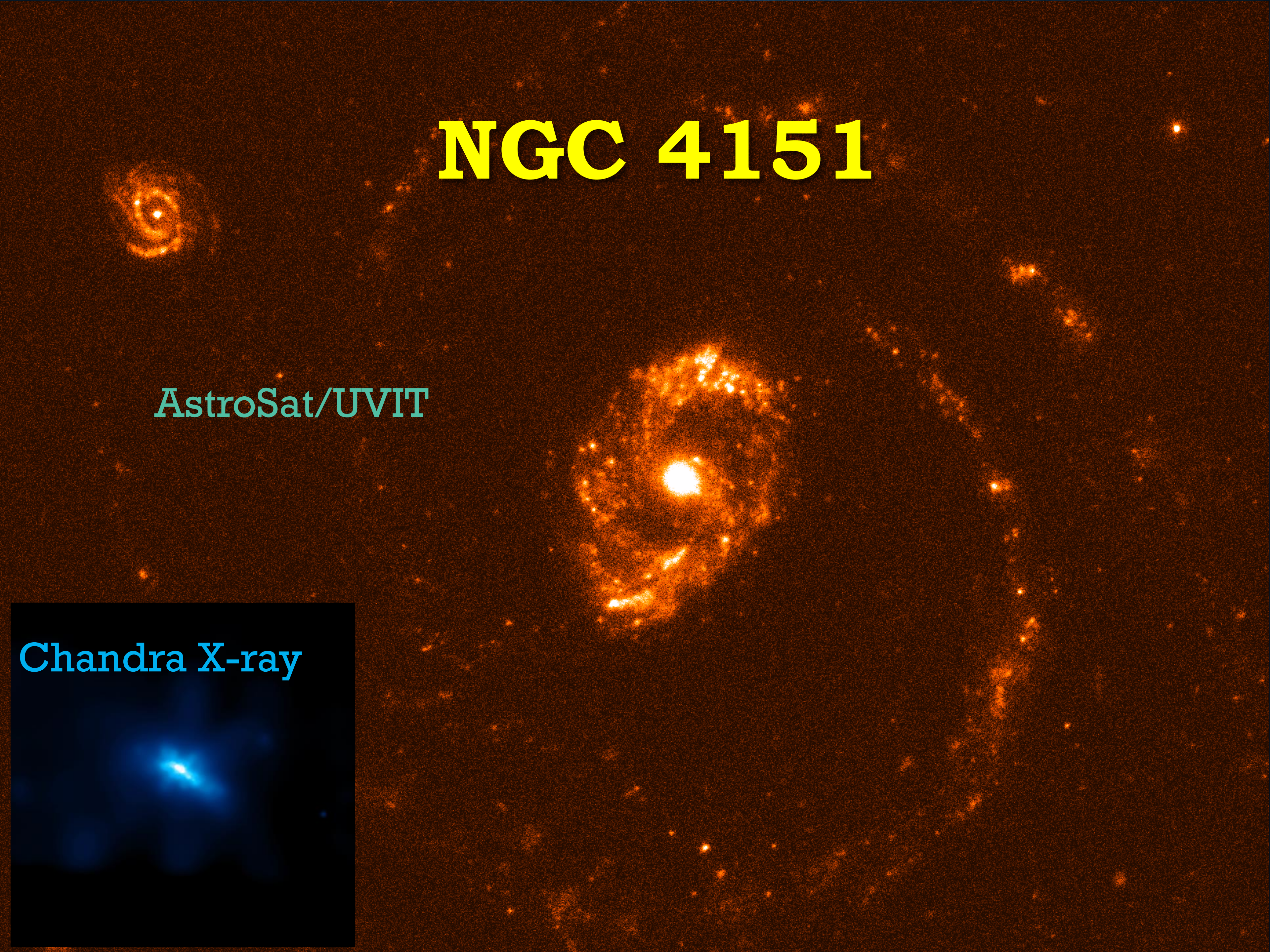
NGC 4151
AstroSat/UVIT
Chandra X-ray

THANKS !